Table 1 Detection results of screening modality for each cancer

Suspected malignancy[a]	Screening modality[b]	Relative sensitivity (%)	PPV (%)
Malignant lymphoma (58/147)	FDG	93.1	38.6
	CT (39)	76.5	48.1
Head and neck cancer (27/332)	FDG	96.2	8.0
	CT (48)	21.1	50.0
	SCC (82)	20.0	7.1
Esophagus cancer (35/85)	FDG	65.7	38.3
	CT (24)	62.5	71.4
	GF (24)	100.0	75.0
Hepatobiliary and gallbladder cancer (37/133)	FDG	78.4	43.9
	CT (37)	75.0	25.0
	US (58)	50.0	80.8
	MR I (36)	41.2	29.2
	AFP (52)	45.5	27.8
Pancreatic cancer (39/115)	FDG	97.4	52.1
	CT (34)	75.0	47.4
	US (67)	50.0	32.4
	MR I (27)	60.0	64.3
	CA19-9 (85)	58.1	66.7
	CEA (83)	47.8	50.0
Renal cell cancer (62/103)	FDG	69.4	70.5
	CT (28)	100.0	57.1
	US (70)	65.9	61.7
	MRI (58)	76.5	72.2
Cervical and uterine cancer (37/148)	FDG	84.2	29.4
	CT (44)	40.0	16.7
	US (59)	35.7	29.4
	MRI (75)	82.4	29.4
	CA125 (97)	12.5	23.1
Ovarian cancer (25/80)	FDG	96.0	41.4
	CT (32)	64.3	42.9
	MRI (32)	94.1	59.3
	US (37)	60.0	46.2
	CA125 (60)	73.7	58.3
Bladder cancer (29/76)	FDG	27.6	100.0
	MRI (29)	63.6	87.5

PPV positive predictive value, *FDG* FDG-PET and FDG-PET/CT

[a] The parentheses represented the number of found cancer/the number of subjects suspected for each type of cancer

[b] The parentheses represented the number of subjects who performed each type of screening modality

(22 cases) and sarcoidosis (10 cases). No malignancy was proven in 28 cases and the other 17 cases were strictly followed because of undeniable possibility of malignancy. Malignant lymphoma was most frequently found in men in the age group of 50–59 years. The final diagnosis of malignancy was confirmed by biopsy (29 cases) and surgical procedures (9 cases). The typical pathological classification of the malignant lymphoma was follicular lymphoma (15 cases), mucosa-associated lymphoid tissue (MALT) lymphoma (9 cases), and diffuse large B cell lymphoma (DLBCL) (6 cases).

The relative sensitivity of FDG-PET or PET/CT for clinical staging according to the Ann Arbor classification was 100.0% (all 10 cases) for Stage I, 100.0% (all 5 cases) for Stage II, 100.0% (all 8 cases) for Stage III, and 100.0% (1 case) for Stage IV.

FDG-PET and PET/CT showed a relative sensitivity of 93.1% and positive predictive value (PPV) of 38.6%. Dedicated PET showed a relative sensitivity of 90.5% (19 of 21 cases) and a PPV of 33.9% (19 of 56 cases). PET/CT showed a relative sensitivity of 94.6% (35 of 37 cases) and a PPV of 41.7% (35 of 84 cases). No significant difference was observed between dedicated PET and PET/CT regarding sensitivity and PPV.

Results of delayed scanning were obtained from 48 cases; 39 cases showed increased accumulation (22 malignant cases), 4 cases showed decreased accumulation (4 benign cases), and 5 cases showed unchanged accumulation (3 malignant cases). The combined examination most adopted with dedicated PET was CT in 39 cases. Computed tomography showed a relative sensitivity of 76.5% (13 of 17 cases) and a PPV of 48.1% (13 of 27 cases).

Head and neck cancer

Among 332 subjects (213 men and 119 women) with a suspicion of head and neck cancer, there were 27 cases of cancer (in 23 men and 4 women) including 13 cases of pharyngeal cancer, 7 cases of laryngeal cancer, 4 cases of salivary gland cancer, 1 case of mandible cancer, 1 case of maxillary cancer, and 1 case of tongue cancer, and 88 cases of benign disease. The most frequently found benign diseases were inflammation (41 cases), Warthin's tumor (16 cases), pleomorphic adenoma (12 cases), and adenoid (9 cases). Head and neck cancer was most frequently found in the age group of 70–79 years. The final diagnosis of malignancy was confirmed by biopsy (16 cases) and surgical procedures (6 cases).

FDG-PET showed a relative sensitivity of 96.2% and PPV of 8.0%. Dedicated PET showed a relative sensitivity of 100.0% (all 12 cases) and a PPV of 8.6% (12 of 140 cases). PET/CT showed a relative sensitivity of 93.3% (14 of 15 cases) and a PPV of 7.5% (14 of 186 cases). No significant difference was observed between dedicated PET and PET/CT regarding sensitivity and PPV.

Results of delayed scanning were obtained from 94 cases; 54 cases were increased accumulation (9 malignant cases), 12 cases were decreased accumulation (12 benign cases), and 28 cases were unchanged accumulation (28 benign cases). The combined examinations most frequently

Table 2 Detection results of PET and PET/CT for each cancer

Malignancy	Screening modality	Relative sensitivity (%)	PPV (%)
Malignant lymphoma (58/147)[a]	PET (58)[b]	90.5	33.9
	PET/CT (89)	94.6	41.7
Head and neck cancer (27/332)	PET (143)	100.0	8.6
	PET/CT (189)	93.3	7.5
Esophagus cancer (35/85)	PET (35)	62.5	52.6
	PET/CT (50)	68.4	31.7
Hepatobiliary and gallbladder cancer (37/133)	PET (69)	70.0	31.8
	PET/CT (64)	81.5	50.0
Pancreatic cancer (39/115)	PET (51)	92.9	54.2
	PET/CT (64)	100.0	51.0
Renal cell cancer (62/103)	PET (44)	42.1	50.0
	PET/CT (59)	81.4	77.8
Cervical and uterine cancer (37/148)	PET (71)	84.6	22.4
	PET/CT (77)	84.0	35.0
Ovarian cancer (25/80)	PET (44)	92.9	50.0
	PET/CT (36)	100.0	34.4
Bladder cancer (29/76)	PET (57)	–	–
	PET/CT (19)	61.5	100.0

PPV positive predictive value

[a] The parentheses represented the number of found cancer/the number of subjects suspected for each type of cancer

[b] The parentheses represented the number of subjects who performed each type of screening modality

Table 3 Results of delayed imaging compare to FDG-PET early imaging

Malignancy	Alternation		
	Increased	No change	Decreased
Malignant lymphoma	56.4 (22/39)	60.0 (3/5)	0.0 (0/4)
Head and neck cancer	16.7 (9/54)	0.0 (0/28)	0.0 (0/12)
Esophagus cancer	85.7 (12/14)	50.0 (2/4)	20.0 (1/5)
Hepatobiliary and gallbladder cancer	58.8 (10/17)	11.1 (1/9)	50.0 (1/2)
Pancreatic cancer	76.2 (16/21)	27.3 (3/11)	0.0 (0/1)
Renal cell cancer	75.0 (3/4)	75.0 (8/12)	100.0 (2/2)
Cervical and uterine cancer	33.3 (8/24)	33.3 (4/12)	16.7 (1/6)
Ovarian cancer	76.5 (13/17)	30.0 (3/10)	0.0 (0/3)

adopted were squamous cell carcinoma (SCC) antigen (82 cases) and CT to dedicated PET (48 cases). SCC antigen showed a relative sensitivity of 20.0% (1 out of 5 cases) and a PPV of 7.1% (1 out of 14 cases). Computed tomography showed a relative sensitivity of 21.1% (4 out of 19 cases) and a PPV of 50.0% (4 out of 8 cases).

Esophageal cancer

Among 85 subjects (62 men and 23 women) with a suspicion of esophageal cancer, 35 cases (29 men and 6 women) of esophageal cancer and 25 cases of benign disease were found. The most frequently found benign disease with dedicated PET- or PET/CT-positive results was esophagitis.

Esophageal cancer was most frequently found in men in the age group of 60–69 years. The final diagnosis of malignancy was confirmed by biopsy (18 cases), surgical procedures (7 cases), and endoscopic mucosal resection (4 cases). The pathological classification of the esophageal cancer was mostly SCC. The relative sensitivity of FDG-PET or PET/CT for clinical staging according to the UICC classification was 12.5% (1 of 8 cases) for Stages 0 and I, 100.0% (all 3 cases) for Stage II, 100.0% (all 2 cases) for Stage III, and 100.0% (one case) for Stage IV.

FDG-PET and PET/CT showed a relative sensitivity of 65.7% and a PPV of 38.3%. Dedicated PET showed a relative sensitivity of 62.5% (10 of 16 cases) and a PPV of 52.6% (10 of 19 cases). PET/CT showed a relative sensitivity of 68.4% (13 of 19 cases) and a PPV of 31.7% (13 of 41 cases). No significant difference was observed between dedicated PET and PET/CT regarding sensitivity and PPV.

Results of delayed scanning were obtained from 23 cases; 14 cases were increased accumulation (12 malignant cases), 5 cases were decreased accumulation (1 malignant case), and 4 cases were unchanged accumulation (2 malignant cases). The combined examinations most frequently adopted were CT to dedicated PET (24 cases) and gastric endoscopy (24 cases). Computed tomography showed a relative sensitivity of 62.5% (5 out of 8 cases) and a PPV of 71.4% (5 out of 7 cases). Gastric endoscopy showed a relative sensitivity of 100.0% (all 18 cases) and a PPV of 75.0% (18 out of 24 cases).

Hepatobiliary and gallbladder cancer

Among 133 subjects (86 men and 47 women) with a suspicion of hepatobiliary cancer and gallbladder cancer, 37 subjects (26 men and 11 women) had proven cancer (23 cases of primary hepatocellular cancer [HCC], 5 cases of bile duct cancer, 6 cases of gallbladder cancer, and 3 cases of metastatic liver cancer); 65 cases of benign disease were found. The most frequently found benign disease was liver hemangioma (28 cases). Cancer was most frequently found in men in the age group of 60–69 years. The final diagnosis of malignancy was confirmed by surgical procedures (17 cases) and biopsy (6 cases).

FDG-PET showed a relative sensitivity of 78.4% and a PPV of 43.9%. Dedicated PET showed a relative sensitivity of 70.0% (7 out of 10 cases) and a PPV of 31.8% (7 out of 22 cases). PET/CT showed a relative sensitivity of 81.5% (22 out of 27 cases) and a PPV of 50.0% (22 out of 44 cases). No significant difference was observed between dedicated PET and PET/CT regarding sensitivity and PPV. Sufficient results of FDG-PET or PET/CT for clinical staging according to the UICC classification were not obtained for hepatobiliary and gallbladder cancer.

Results of delayed scanning were obtained from 29 cases; 17 cases showed increased accumulation (10 malignant cases), 9 cases showed unchanged accumulation (1 malignant case), and 2 cases showed decreased accumulation (1 malignant case). The combined examinations most frequently adopted were CT to dedicated PET (40 cases), abdominal MRI (39 cases), and abdominal ultrasonography (61 cases). Computed tomography showed a relative sensitivity of 75.0% (6 out of 8 cases), and a PPV of 25.0% (6 out of 24 cases). Abdominal MRI showed a relative sensitivity of 41.2% (7 out of 17 cases) and a PPV of 29.2% (7 out of 24 cases). Abdominal ultrasonography showed a relative sensitivity of 50.0% (21 of 42 cases) and a PPV of 80.0% (21 out of 26 cases). The primary combined tumor marker for cases with suspected hepatic cancer was α-fetoprotein (AFP) (52 cases), which showed a relative sensitivity of 45.5% (5 out of 11 cases) and a PPV of 27.8% (5 out of 18 cases).

Pancreatic cancer

Among 115 subjects (65 men and 50 women) with a suspicion of pancreatic cancer, 38 cases (20 men and 18 women) of pancreatic cancer, 1 case of malignant islet cell tumor, and 23 cases of benign disease were found. The most frequently found disease other than the 38 cases of malignancy was intraductal papillary mucinous neoplasm (11 cases).

Pancreatic cancer was most frequently found in the age group of 70–79 years. The final diagnosis of malignancy was confirmed by surgical procedures (12 cases), biopsy (7 cases), and cytological diagnosis (4 cases). The pathological classification of the pancreatic carcinoma was mostly adenocarcinoma. The relative sensitivity of FDG-PET or PET/CT for clinical staging according to the UICC classification was 100.0% (all 4 cases) for Stage I, 100.0% (all 2 cases) for Stage II, 100.0% (all 3 cases) for Stage III, and 100.0% (all 6 cases) for Stage IV.

FDG-PET and PET/CT showed a relative sensitivity of 97.4% and a PPV of 52.1%. Dedicated PET showed a relative sensitivity of 92.9% (13 of 14 cases) and a PPV of 54.2% (13 of 24 cases). PET/CT showed a relative sensitivity of 100.0% (all 25 cases) and a PPV of 51.0% (25 of 49 cases). No significant difference was observed between dedicated PET and PET/CT regarding sensitivity and PPV.

Results of delayed scanning were obtained from 33 cases; 21 cases showed increased accumulation (16 malignant cases), 1 case showed decreased accumulation (1 benign case), and 11 cases showed unchanged accumulation (3 malignant cases). The combined examinations most frequently adopted were ultrasonography (67 cases), CT to dedicated PET (34 cases), and abdominal MRI (27 cases). Abdominal ultrasonography showed a relative sensitivity of 50.0% (12 out of 24 cases) and a PPV of 32.4% (12 out of 37 cases). Computed tomography showed a relative sensitivity of 75.0% (9 out of 12 cases), and a PPV of 47.4% (9 out of 19 cases). Abdominal MRI showed a relative sensitivity of 60.0% (9 out of 15 cases) and a PPV of 64.3% (9 out of 14 cases). The cancer antigen 19-9 (CA19-9) showed a relative sensitivity of 58.1% (18 out of 31 cases) and a PPV of 66.7% (9 out of 19 cases), and carcinoembryonic antigen (CEA) showed a relative sensitivity of 47.8% (11 out of 23 cases) and a PPV of 50.0% (11 out of 22 cases).

Renal cell cancer

Among 103 subjects (75 men and 28 women) with a suspicion of renal cell cancer, 62 cases (48 men and 14 women) of renal cell carcinoma and 20 cases of benign disease were found. The most frequently found benign disease was renal cyst (11 cases). Renal cell carcinoma was most frequently found in the age group of 50–59 years. The final diagnosis of malignancy was confirmed by surgical procedures (51 cases) and biopsy (2 cases). The pathological classification of the renal cell carcinoma was mostly clear cell carcinoma. The relative sensitivity of FDG-PET or PET/CT for pathological staging according to the UICC classification was 57.1% (12 of 21 cases) for Stage I, 66.7% (2 of 3 cases) for Stage II, and 100.0% (all 2 cases) for Stage III.

FDG-PET and PET/CT showed a relative sensitivity of 69.4% and a PPV of 70.5%. Dedicated PET showed a

relative sensitivity of 42.1% (8 out of 19 cases) and a PPV of 50.0% (8 out of 16 cases). PET/CT showed a relative sensitivity of 81.4% (35 out of 43 cases) and a PPV of 77.8% (35 out of 45 cases). PET/CT had a higher sensitivity ($P < 0.01$) and PPV than dedicated PET ($P < 0.05$).

Results of delayed scanning were obtained from 18 cases; 4 cases showed increased accumulation (3 malignant cases), 2 cases showed decreased accumulation (both malignant), and 12 cases showed unchanged accumulation (8 malignant cases). The combined examinations most frequently adopted were abdominal ultrasonography (70 cases), abdominal MRI (59 cases), and CT to dedicated PET (28 cases). Abdominal ultrasonography showed a relative sensitivity of 65.9% (29 out of 44 cases) and a PPV of 61.7% (29 of 47 cases). Abdominal MRI showed a relative sensitivity of 76.5% (13 out of 17 cases) and a PPV of 77.2% (13 out of 18 cases). Computed tomography showed a relative sensitivity of 100.0% (all 12 cases) and a PPV of 57.1% (12 out of 21 cases).

Cervical and uterine cancer

Among 148 women with a suspicion of cervical and uterine cancer, 23 cases of uterine body cancer, 12 cases of uterine cervix cancer, 2 cases of uterine sarcoma, and 63 cases of benign disease were found. The most frequently found benign disease was leiomyoma of the uterus (45 cases).

Cervical and uterine cancer was most frequently found in the age group of 50–59 years. The final diagnosis of malignancy was confirmed by surgical procedures (24 cases) and biopsy (8 cases). The relative sensitivity of FDG-PET or PET/CT for pathological staging according to the UICC classification was 90.0% (9 of 10 cases) for Stage I, 100.0% (all 4 cases) for Stage II, 100.0% (all 3 cases) for Stage III, and 100.0% (one case) for Stage IV.

FDG-PET and PET/CT showed a relative sensitivity of 84.2% and a PPV of 29.4%. Dedicated PET showed a relative sensitivity of 84.6% (11 of 13 cases) and a PPV of 22.4% (11 out of 49 cases). PET/CT showed a relative sensitivity of 84.0% (21 out of 25 cases), and a PPV of 35.0% (21 out of 60 cases). No significant difference was observed between dedicated PET and PET/CT regarding sensitivity and PPV.

Results of delayed scanning were obtained from 42 cases; 24 cases showed increased accumulation (8 malignant cases), 6 cases showed decreased accumulation (1 malignant case), and 12 cases showed unchanged accumulation (4 malignant cases). The combined examinations most commonly adopted were pelvic MRI (75 cases), pelvic ultrasonography (59 cases), and CT to dedicated PET (44 cases). Pelvic MRI showed a relative sensitivity of 82.4% (14 out of 17 cases), and a PPV of 26.4% (14 out of 53 cases). Pelvic ultrasonography showed a relative sensitivity of 35.7% (5 out of 14 cases), and a PPV of 29.4% (5 out of 17 cases). Computed tomography showed a relative sensitivity of 40.0% (2 out of 5 cases) and a PPV of 16.7% (2 out of 12 cases). The primary combined tumor marker was cancer antigen 125 (CA125) (97 cases), which showed a relative sensitivity of 12.5% (3 out of 24 cases) and a PPV of 23.1% (3 out of 13 cases). Papanicolaou smear and human papilloma virus screening were not performed.

Ovarian cancer

Among 80 women with a suspicion of ovarian cancer, 25 cases of ovarian cancer and 19 cases of benign disease were found. The most frequently found benign disease was ovarian cyst (13 cases). Ovarian cancer was most frequently found in the age group of 50–59 years. The final diagnosis of malignancy was confirmed by surgical procedures (20 cases). The pathological classification of the ovarian carcinoma was mostly mutinous cyst adenocarcinoma (17 cases). The result of FDG-PET or PET/CT for clinical staging according to the pathological UICC classification was 100.0% (all 4 cases) for Stage I, 66.7% (2 of 3 cases) for Stage II, and 100.0% (all 2 cases) for Stage III.

FDG-PET showed a relative sensitivity of 96.0% and a PPV of 41.4%. Dedicated PET showed a relative sensitivity of 92.9% (13 out of 14 cases) and a PPV of 50.0% (13 out of 26 cases). PET/CT showed a relative sensitivity of 100.0% (all 11 cases) and a PPV of 34.4% (11 out of 32 cases). No significant difference was observed between dedicated PET and PET/CT regarding sensitivity and PPV.

Results of delayed scanning were obtained from 30 cases; 17 cases showed increased accumulation (13 malignant cases), 3 cases showed decreased accumulation (3 malignant cases), and 10 cases showed unchanged accumulation (3 malignant cases). The combined examinations most frequently adopted were CT to dedicated PET (32 cases), pelvic MRI (32 cases), and pelvic ultrasonography (37 cases). Computed tomography showed a relative sensitivity of 64.3% (9 out of 14 cases) and a PPV of 42.9% (9 out of 21 cases). Pelvic MRI showed a relative sensitivity of 94.1% (16 out of 17 cases) and a PPV of 59.3% (16 out of 27 cases). Pelvic ultrasonography showed a relative sensitivity of 60.0% (6 out of 10 cases) and a PPV of 46.2% (6 out of 13 cases). The primary combined tumor marker was CA125 (60 cases), which showed a relative sensitivity of 73.7% (14 out of 19 cases) and a PPV of 58.3% (14 out of 24 cases).

Bladder cancer

Among 76 subjects (41 men and 35 women) with a suspicion of bladder cancer, 29 cases of cancer (all in men) were found. Most subjects were proven to be without any disease. Cancer was only found in men in the age group of

60–69 years. The final diagnosis of malignancy (28 cases) was confirmed by tissue diagnosis with transurethral resection or biopsy. The results of FDG-PET or PET/CT for clinical staging according to the pathological UICC classification were 18.2% (2 out of 11 cases) for Stage I.

FDG-PET showed a relative sensitivity of 27.6% and a PPV of 100.0%. Dedicated PET showed no cases of PET-positive findings. PET/CT showed a relative sensitivity of 61.5% (8 out of 13 cases) and a PPV of 100.0% (all 8 cases). Most of the positive findings in PET/CT were confirmed by the CT portion of PET/CT (7 out of 8 cases).

Delayed scanning was not performed in most of the cases. The combined examination most frequently adopted was pelvic MRI (29 cases). Pelvic MRI showed a relative sensitivity of 63.6% (14 out of 22 cases) and a PPV of 87.5% (14 out of 16 cases).

Discussion

The FDG-PET cancer screening program has contributed to the detection of various types of malignant neoplasms because it is a FDG-PET- and PET/CT-centered program supported by combined screening examination for screening FDG-negative malignant neoplasms [2, 3, 6, 7]. This is the most distinctive feature of the FDG-PET cancer screening program and it has the possibility of comprehensive cancer screening. Several kinds of malignant neoplasms have no definitive screening methods; thus, this screening program may have the potential to cover a wide variety of malignant neoplasms. The previous reports showed that numerous malignant neoplasms were found by this cancer screening program [2, 3, 6, 7].

The estimated peak age of patients diagnosed with malignant neoplasm was in the age group of 70–79 years in Japan, and over 50% of patients with malignant neoplasms were categorized in age group of 70–79 years and 80 years and older [8]. The peak age of malignant neoplasms detected in FDG-PET cancer screening program was age group of 60–69 years, and 67% of cancer detected was in age group of 50–59 years and 60–69 years. Although malignant neoplasms were found earlier in FDG-PET cancer screening program than in Japanese statistical survey, it was insufficient to discuss the utility of FDG-PET cancer screening program due to lead-time bias [9].

A feature of the malignant lymphoma detected in the screening program was that it was of the indolent type, as were follicular lymphoma and MALT. This cancer screening program targeted asymptomatic subjects, so few cases of aggressive type lymphoma, such as DLBCL, were expected to be found. The clinical stage according to the Ann Arbor classification of the malignant lymphoma found varied, possibly due to the capability of entire body screening by FDG-PET and PET/CT at one time. The difference in the detection rate was not statistically significant between dedicated PET and PET/CT. Because the indolent type of malignant lymphoma has generally low FDG accumulation [10], it may cause the low screening specificity. A recent study showed the advantage of PET/CT compared to dedicated PET in the indolent type of lymphoma [11].

In this screening program, there were many cases of suspected head and neck cancer. Dedicated PET and PET/CT had a high sensitivity in detecting cancers, but extremely low specificity for detecting head and neck cancer. This was due to the physiological accumulation of FDG in the oral and pharyngeal spaces. Even if localized or asymmetric FDG accumulation was one of the features to distinguish true positive cases from nonspecific FDG accumulation [12] and it was closely reviewed in the guideline of FDG-PET cancer screening, further study is needed to establish more specific diagnostic guidelines.

Screening for early esophageal cancer was limited in this program. The detection rate was not different between dedicated PET and PET/CT, while these utilities are limited for the advanced stage [13, 14]. A survey with gastric endoscopy had reliably and accurately screened esophageal cancer. We showed the high contribution of gastric endoscopy for screening gastric cancer in a FDG-PET cancer screening program; thus, esophageal cancer should be screened in a series of gastric cancer screenings by gastric endoscopy.

FDG uptake in HCC was variable, because HCC generally had glucose-6-phosphatase activity to dephosphorylation of intercellular FDG-6 phosphatase, causing leakage of FDG back to the circulation [15]. This indicates that some useful screening modality should be combined with FDG-PET or PET/CT. The standard modality for hepatic imaging has been dual phase (arterial and portal) contrast CT, ultrasonography, and MRI [16]. Because contrast material is not basically used in a cancer screening program, a hepatic lesion was inevitably evaluated by a noncontrast image, regardless of the known disadvantage. It appeared that abdominal ultrasonography was the expecting screening modality to cover FDG-PET and PET/CT; however, it should be considered that ultrasonography is highly dependent on operator skill and patient physique. Patients infected with the hepatitis B or C virus (HBV, HCV) are at high risk for the development of HCC [17]; thus, it may be a useful test for screening hepatic cancer even if few facilities have adopted HBV and/or HCV in their screening program. Elevated serum alpha-fetoprotein (AFP) was seen in patients with HCC, while it depended on the AFP threshold [18]. On the other hand, serum AFP has no evidence of usefulness in an HCC screening for an asymptomatic population. Thus, AFP should be referred in subjects who have hepatic cirrhosis and/or a suspicion of a sizeable mass lesion in the liver [19, 20].

Regarding the screening for pancreatic cancer, dedicated PET and PET/CT had a high contribution for detection and a slight advantage over CT alone. The clinical stage of pancreatic cancer detected was deviation to advanced stage, which indicated the difficulty of screening pancreatic cancer even in asymptomatic subjects, because it generally has poor prognosis [21]. The sensitivity of FDG-PET for pancreas cancer did not depend on lesion size with diameter of over 1 cm [22]. Moreover, the sensitivity for Stage I pancreas cancer did not differ between FDG-PET and CT [23]. However, it was necessary to consider the possibility of small pancreas lesion with false negative in this cancer screening program. Because 60% of pancreas cancer was advanced type [24], even small pancreas lesions can lead to bad prognosis. CA19-9 and CEA were the representative serum tumor markers for a pancreatic tumor, but they are not cancer- or organ-specific [25]. One study on screening pancreatic cancer in 10,000 asymptomatic subjects using ultrasonography or CA19-9 resulted in an extremely low PPV of 0.5% [26]. Further study is needed to compare the prognosis of asymptomatic pancreatic cancer found by this screening program with that found by other screening programs.

The FDG-PET imaging of primary renal cell carcinoma was limited, because renal cell carcinoma tended to show low FDG accumulation and was interfered with by FDG excretion [27]. The standard evaluation for renal cell carcinoma has been contrast-enhanced CT [28]. However, the CT contrast medium is not used for the cancer screening program. Our result showed low sensitivity of dedicated PET for screening renal cell carcinoma but quite high sensitivity of PET/CT. For screening renal cell carcinoma, dedicated CT or the CT portion of PET/CT should be incorporated into the screening program.

Both dedicated PET and PET/CT had high sensitivity for screening gynecological cancers. FDG-PET was well known to have limitations for assessing the parametrial invasion of gynecological cancer [29, 30]; moreover, for benign diseases such as leiomyoma of the uterus and premenopausal state, which often showed FDG accumulation [31–33], pelvic MRI should be combined with FDG-PET or PET/CT, even if the result of MRI findings for these cancers is nearly identical to dedicated PET and PET/CT. In this survey, serum CA125 contributed to the screening of ovarian cancer, but had a lower advantage for cervical and uterine cancer. Ovarian cancer screening by serum CA125 alone resulted in a PPV of 0.03% [34], but combined screening with serum CA125 contributed to increasing the diagnostic value of FDG-PET [35].

FDG-PET had no diagnostic value for screening bladder cancer because excreted FDG accumulated in the bladder. In contrast, pelvic MRI had good results in screening bladder cancer; thus, pelvic MRI was recommended for checking for bladder lesions. A hematuria screening was performed in several facilities but it was expected to be of little value because one study with a retrospective review of 20,000 subjects showed only one case of bladder cancer [36].

The delayed scanning of FDG-PET had the ability to distinguish malignant from nonmalignant regions and the increased accumulation of FDG in delayed scanning had a higher possibility of identifying an existing malignancy [37]. Our results showed that increased FDG accumulation in delayed scanning compared to early imaging had a quite high prevalence of malignancy and many cases had proven malignancy even with unchanged FDG accumulation in delayed scanning compared to early imaging. The alternation of FDG accumulation in delayed scanning can be an index to eliminate a high-risk group of malignancy. However, the burden of delayed imaging was different with each type of cancer; the head and neck region and the cervical and uterine region had low prevalence of cancer, which might indicate that true lesions are indistinguishable from physiological FDG uptake. In addition, several cases were proved to be malignant with decreasing accumulation in delayed scanning; thus, the limitation of this index must always be taken into consideration.

Conclusions

We analyzed various types of malignant neoplasms found by a FDG-PET cancer screening program. A statistically significant difference in the screening results between PET/CT and PET was found in screening renal cell carcinoma even if the results of PET/CT was prior to those of PET in all types of malignant neoplasms. The results of the FDG-PET screening program showed that malignant lymphoma was frequently found to be the indolent type, more specific diagnostic criteria were needed for screening head and neck cancer, and that pancreatic cancer in asymptomatic subjects was most often in the advanced stage. The recommended modality for combined screening with PET or PET/CT was gastric endoscopy for covering early esophageal cancer, abdominal ultrasonography for checking hepatobiliary and gallbladder cancer, pelvic magnetic resonance imaging for assessing gynecological and pelvic cancer, and a CA125 blood test for screening ovarian cancer. The delayed scanning was helpful for the screening program; however, it was dependent on the type of suspected malignant neoplasm.

Acknowledgments This research was supported by management expenses grants from the government to the national cancer center No.21-5-2. The authors thank the Japan Radioisotope Association Division of Medical and Pharmaceutical Drugs.

References

1. Yeung HW, Schöder H, Smith A, Gonen M, Larson SM. Clinical value of combined positron emission tomography/computed tomography imaging in the interpretation of 2-deoxy-2-[F-18]fluoro-D-glucose-positron emission tomography studies in cancer patients. Mol Imaging Biol. 2005;7:229–35.
2. Ide M. Cancer screening with FDG-PET. Q J Nucl Med Mol Imaging. 2006;50:23–7.
3. Minamimoto R, Senda M, Uno K, Jinnouchi S, Iinuma T, Ito K, et al. Performance profile of FDG-PET and PET/CT for cancer screening on the basis of a Japanese Nationwide Survey. Ann Nucl Med. 2007;21:481–98.
4. The guideline of FDG-PET cancer screening. Kaku Igaku. 2004; 41:1–21.
5. The guideline of FDG-PET cancer screening 2007. Kaku Igaku. 2007; 44:1–28.
6. Kojima S, Zhou B, Teramukai S, Hara A, Kosaka N, Matsuo Y, et al. Cancer screening of healthy volunteers using whole-body 18F-FDG-PET scans: the Nishidai clinic study. Eur J Cancer. 2007;43:1842–8.
7. Nishizawa S, Kojima S, Teramukai S, Inubushi M, Kodama H, Maeda Y, et al. Prospective evaluation of whole-body cancer screening with multiple modalities including [18F]fluorodeoxyglucose positron emission tomography in a healthy population: a preliminary report. J Clin Oncol. 2009;27:1767–73.
8. The Foundation of Cancer Research (FPCR). Cancer Statistics in Japan, 2009.
9. Schöder H, Gönen M. Screening for cancer with PET and PET/CT: potential and limitations. J Nucl Med. 2007;48(Suppl 1):4S–18S.
10. Schöder H, Noy A, Gönen M, Weng L, Green D, Erdi YE, et al. Intensity of 18fluorodeoxyglucose uptake in positron emission tomography distinguishes between indolent and aggressive non-Hodgkin's lymphoma. J Clin Oncol. 2005;23:4643–51.
11. Fueger BJ, Yeom K, Czernin J, Sayre JW, Phelps ME, Allen-Auerbach MS. Comparison of CT, PET, and PET/CT for staging of patients with indolent non- Hodgkin's lymphoma. Mol Imaging Biol. 2009;11:269–74.
12. Wahl RL. Principles and practice of PET and PET/CT. 2nd ed. Lippincott Williams & Wilkins; 2009. p. 221–39.
13. Flamen P, Lerut A, Van Cutsem E, De Wever W, Peeters M, Stroobants S, et al. Utility of positron emission tomography for the staging of patients with potentially operable esophageal carcinoma. J Clin Oncol. 2000;18:3202–10.
14. Ott K, Weber WA, Fink U, Helmberger H, Becker K, Stein HJ, et al. Fluorodeoxyglucose-positron emission tomography in adenocarcinomas of the distal esophagus and cardia. World J Surg. 2003;27:1035–9.
15. Weber G, Morris HP. Comparative biochemistry of hepatomas. III. Carbohydrate enzymes in liver tumors of different growth rates. Cancer Res. 1963;23:987–94.
16. De Santis M, Romagnoli R, Cristani A, Cioni G, Casolo A, Vici FF, et al. MRI of small hepatocellular carcinoma: comparison with US, CT, DSA, and Lipiodol-CT. J Comput Assist Tomogr. 1992;16:189–97.
17. Yoon SK. Recent advances in tumor markers of human hepatocellular carcinoma. Intervirology. 2008;51(Suppl 1):34–41.
18. Stefaniuk P, Cianciara J, Wiercinska-Drapalo A. Present and future possibilities for early diagnosis of hepatocellular carcinoma. World J Gastroenterol. 2010;16:418–24.
19. Nomura F, Ohnishi K, Tanabe Y. Clinical features and prognosis of hepatocellular carcinoma with reference to serum alpha-fetoprotein levels. Analysis of 606 patients. Cancer. 1989;64:1700–7.
20. Trevisani F, D'Intino PE, Morselli-Labate AM, Mazzella G, Accogli E, Caraceni PJ, et al. Serum alpha-fetoprotein for diagnosis of hepatocellular carcinoma in patients with chronic liver disease: influence of HBsAg and anti-HCV status. J Hepatol. 2001;34:570–5.
21. Beger HG, Rau B, Gansauge F, Poch B, Link KH. Treatment of pancreatic cancer: challenge of the facts. World J Surg. 2003; 27:1075–84.
22. Rose DM, Delbeke D, Beauchamp RD, Chapman WC, Sandler MP, Sharp KW, et al. 18Fluorodeoxyglucose-positron emission tomography in the management of patients with suspected pancreatic cancer. Ann Surg. 1999;229:729–37 (discussion).
23. Delbeke D, Rose DM, Chapman WC, Pinson CW, Wright JK, Beauchamp RD, et al. Optimal interpretation of FDG PET in the diagnosis, staging and management of pancreatic carcinoma. J Nucl Med. 1999;40:1784–91.
24. Wahl RL. Principles and practice of PET and PET/CT. 2nd ed. Lippincott Williams & Wilkins; 2009. p. 331–47.
25. Steinberg WM, Gelfand R, Anderson KK, Glenn J, Kurtzman SH, Sindelar WF, et al. Comparison of the sensitivity and specificity of the CA19–9 and carcinoembryonic antigen assays in detecting cancer of the pancreas. Gastroenterology. 1986;90:343–9.
26. Homma T, Tsuchiya R. The study of the mass screening of persons without symptoms and of the screening of outpatients with gastrointestinal complaints or icterus for pancreatic cancer in Japan, using CA19-9 and elastase-1 or ultrasonography. Int J Pancreatol. 1991;9:119–24.
27. Montravers F, Grahek D, Kerrou K, Younsi N, Doublet JD, Gattegno B, et al. Evaluation of FDG uptake by renal malignancies (primary tumor or metastases) using a coincidence detection gamma camera. J Nucl Med. 2000;41:78–84.
28. Kopka L, Fischer U, Zoeller G, Schmidt C, Ringert RH, Grabbe E. Dual-phase helical CT of the kidney: value of the corticomedullary and nephrographic phase for evaluation of renal lesions and preoperative staging of renal cell carcinoma. AJR Am J Roentgenol. 1997;169:1573–8.
29. Wahl RL. Principles and practice of PET and PET/CT. 2nd ed. Lippincott Williams & Wilkins; 2009. p. 348–54.
30. Chao A, Chang TC, Ng KK, Hsueh S, Huang HJ, Chou HH, et al. 18F-FDG PET in the management of endometrial cancer. Eur J Nucl Med Mol Imaging. 2006;33:36–44.
31. Nishizawa S, Inubushi M, Kido A, Miyagawa M, Inoue T, Shinohara K, et al. Incidence and characteristics of uterine leiomyomas with FDG uptake. Ann Nucl Med. 2008;22:803–10.
32. Kitajima K, Murakami K, Yamasaki E, Kaji Y, Sugimura K. Standardized uptake values of uterine leiomyoma with 18F-FDG PET/CT: variation with age, size, degeneration, and contrast enhancement on MRI. Ann Nucl Med. 2008;22:505–12.
33. Lerman H, Metser U, Grisaru D, Fishman A, Lievshitz G, Even-Sapir E. Normal and abnormal 18F-FDG endometrial and ovarian uptake in pre- and postmenopausal patients: assessment by PET/CT. J Nucl Med. 2004;45:266–71.
34. Einhorn N, Sjövall K, Knapp RC, Hall P, Scully RE, Bast RC Jr, et al. Prospective evaluation of serum CA 125 levels for early detection of ovarian cancer. Obstet Gynecol. 1992;80:14–8.
35. Risum S, Høgdall C, Loft A, Berthelsen AK, Høgdall E, Nedergaard L, et al. The diagnostic value of PET/CT for primary ovarian cancer–a prospective study. Gynecol Oncol. 2007;105: 145–9.
36. Hiatt RA, Ordoñez JD. Dipstick urinalysis screening, asymptomatic microhematuria, and subsequent urological cancers in a population-based sample. Cancer Epidemiol Biomarkers Prev. 1994;3:439–43.
37. Kubota K, Itoh M, Ozaki K, Ono S, Tashiro M, Yamaguchi K, et al. Advantage of delayed whole-body FDG-PET imaging for tumour detection. Eur J Nucl Med. 2001;28:696–703.

PET/CT Allows Stratification of Responders to Neoadjuvant Chemotherapy for High-Grade Sarcoma

A Prospective Study

Ukihide Tateishi, MD, Akira Kawai, MD,† Hirokazu Chuman, MD,† Fumihiko Nakatani, MD,† Yasuo Beppu, MD,† Kunihiko Seki, MD,‡ Mototaka Miyake, MD,§ Takashi Terauchi, MD,¶ Noriyuki Moriyama, MD,¶ and E. Edmund Kim, MD‖*

Purpose: The aim of the present study was to determine whether metabolic reduction is capable of reflecting the histopathologic response and outcome after neoadjuvant chemotherapy in patients with high-grade sarcoma.

Patients and Methods: Forty-two patients with histologically proven high-grade sarcoma underwent neoadjuvant chemotherapy followed by surgical resection. Quantitative F-18 fluorodeoxyglucose (F-18-FDG) positron emission tomography (PET)/computed tomography scans were acquired before and after the first cycle and after completion of neoadjuvant chemotherapy. Standardized uptake values (SUVs) and metabolic reduction rates were compared with histopathologic response, progression-free survival, and overall survival.

Results: Baseline SUVmax was 10.9 ± 3.6 (range, 3.8–19.6). Therapeutic effect resulted in 10 patients (24%) with a satisfactory response and in 32 patients (76%) with an unsatisfactory response after completion of neoadjuvant chemotherapy. The SUV decreased to 7.8 ± 3.4 after the first cycle (t1) of chemotherapy and to 5.2 ± 3.4 after completion (t2) of chemotherapy. Histopathologic response and percentage SUV (t2) reduction rate were independent predictors of progression-free survival and overall survival in the multivariate analyses.

Conclusion: Metabolic reduction after neoadjuvant chemotherapy evaluated by F-18 FDG PET or computed tomography can be used for stratification of the histopathologic response in patients with high-grade sarcoma.

Key Words: PET/CT, sarcoma, neoadjuvant chemotherapy

(*Clin Nucl Med* 2011;36: 526–532)

The majority of patients with high-grade sarcomas are found to have locally advanced tumors at the time of the initial diagnosis. However, surgical resection of the tumors often results in inadequate margin, and there is a high propensity to develop local recurrence and distant metastasis.[1–3]

For patients with high-grade sarcoma, the main treatment option with the potential cure is definitive neoadjuvant chemotherapy followed by surgery. Induction treatment protocols using preoperative chemotherapy or combined chemoradiotherapy followed by resection yield a complete remission rate of 59% at 5 years in high-grade sarcoma.[4–8] Neoadjuvant chemotherapy is under investigation for the treatment of high-grade sarcomas. Prior studies have demonstrated that neoadjuvant chemotherapy followed by standard surgery is associated with comparative response.[4–8]

Imaging metabolic activity offers an alternative method of visualizing the effects of treatment. Malignant transformation of cells is frequently associated with increased metabolic activity. Positron emission tomography (PET) using F-18 fluorodeoxyglucose (F-18 FDG) has been used to evaluate the prognosis in patients with sarcomas.[9–12] The glucose analog F-18 FDG reflects exogenous glucose consumption, because it is phosphorylated by intracellular hexokinases through glucose transporter proteins. F-18 FDG uptake expressed semi-quantitatively as the standardized uptake value (SUV) has been found to be strongly associated with outcome.[13–15] The degree of F-18 FDG uptake in sarcomas is associated with histologic tumor aggressiveness and glucose transporter protein 1 expression.[16,17] Identification of PET findings that affect the prognosis of patients with high-grade sarcoma may be useful to determine preoperative value.

Several studies have revealed that reduction in tumor metabolism often occurs early in the course of therapy and precedes with the reduction of tumor size. Conventional methods for monitoring of treatment response are based on size reduction as revealed by computed tomography (CT). However, CT is not an accurate basis for predicting outcome, because morphologic changes in tumors occur much later than the changes in metabolic response.[6–8] Quantification of tumor glucose metabolism is a highly accurate method of monitoring the effects of chemotherapy.[18–21] Recent studies have revealed that sequential F-18 FDG PET scans are sensitive to detect early response to chemotherapy in malignant tumors.[22–31] The reduction rate of F-18 FDG uptake technique reflects the histopathologic response to chemotherapy.

However, the role of sequential F-18 FDG PET scans in measuring the reduction of metabolic response after neoadjuvant chemotherapy in high-grade sarcomas has not been fully elucidated. The PET/CT can improve the diagnostic accuracy in patients with sarcomas because they record anatomic and molecular information simultaneously. Our hypothesis is that a sequential F-18 FDG PET/CT scans reflect the changes of metabolic process that may be related to the therapeutic response. The purpose of the present study was to clarify whether F-18 FDG PET/CT scans are capable of reflecting the histopathologic response and outcome after neoadjuvant chemotherapy of high-grade sarcomas.

PATIENTS AND METHODS

Patients

All patients underwent initial staging based on a review of their medical history, physical examinations, and imaging studies,

Received for publication August 2, 2010; revision accepted November 7, 2010.

From the *Department of Radiology, Yokohama City University Graduate School of Medicine, Yokohama, Japan; Division of †Orthopedics, ‡Pathology, and §Diagnostic Radiology, National Cancer Center Hospital, Tokyo; ¶Division of Cancer Screening, Research Center for Cancer Prevention and Screening, National Cancer Center, Tokyo; and ‖Division of Diagnostic Imaging, University of Texas, MD Anderson Cancer Center, Houston, TX.

Supported in part by grants from Scientific Research Expenses for Health and Welfare Programs and the Grant-in-Aid for Cancer Research from the Ministry of Health, Labor and Welfare.

The authors declare that they have no conflict of interest.

Reprints: Ukihide Tateishi, MD, Department of Radiology, Yokohama City University Graduate School of Medicine, 3–9, Fukuura, Kanazawa-ku, Yokohama, Kanagawa, 236–0004. Japan. E-mail: utateish@yokohama-cu.ac.jp.

ISSN: 0363-9762/11/3607-0526

including PET/CT. The criteria for eligibility were histologically proven or highly suggestive high-grade soft-tissue sarcoma without any treatment before the study, age greater than 20 years, and adequate organ function. The inclusion criteria for performance status (PS) were PS 0, that is, fully active, able to perform all predisease activities without restriction or PS 1, that is, physically strenuous activity restricted but ambulatory and able to carry out work of a light or sedentary nature.[32] The exclusion criteria were diabetes and pregnancy. Patients who presented with metastatic disease or concomitant malignancy were ineligible according to the protocol. This study was conducted in accordance with the amended Helsinki declaration and approved by the local ethics committees after all the patients had given informed consent.

Treatment

The neoadjuvant therapy consisted of 2 cycles of ifosfamide (10 g/m^2) followed by 2 cycles of doxorubicin (60 mg/m^2) and cisplatin (80 mg/m^2). After completion of the neoadjuvant chemotherapy, all patients underwent surgical resection. All specimens were analyzed by one pathologist, who was blinded to the PET/CT data. According to the criteria based on the histopathologic response, histopathologic responders received adjuvant chemotherapy after surgery with the following regimen: 3 cycles of ifosfamide (10 g/m^2) followed by doxorubicin (60 mg/m^2) and cisplatin (80 mg/m^2). Histopathologic nonresponders received 4 cycles of the same regimen. During the postoperative follow-up, 9 (21%) patients who had developed localized bone metastasis received external beam radiation therapy.

PET/CT

Patients received an intravenous injection of 380 to 401 MBq of F-18 FDG after at least 6 hours of fasting, followed by an uptake phase of approximately 60 minutes. Studies were performed with a lutetium oxyorthosilicate-based whole-body PET/CT scanner (Aquiduo, Toshiba Medical Systems). Data acquisition was performed for each patient from the top of the skull to the leg at a scan length of 120 seconds per one bed position. A total of 10 to 12 bed positions, which depend on the patient's height, were needed for whole-body scans, and the total examination time was approximately 30 minutes. All PET images were reconstructed using an iterative algorithm: attenuation-weighted ordered-subsets expectation maximization, 4 iterations; 14 subsets; 7-mm Gaussian filter. All reconstructed images were reviewed and analyzed on a Voxbase SP1000 workstation (J-MAC systems).

Image Interpretation

PET and CT images in all standard planes were reviewed on the workstation (e-soft, Siemens). Images were analyzed visually and quantitatively by 2 reviewers who recorded their findings after reaching a consensus. Reviewers were blinded to the results of other modalities. In the visual analysis, abnormal F-18 FDG uptake was defined as substantially greater activity than in aortic blood on attenuation-corrected images. A region of interest (ROI) was outlined within areas of increased F-18 FDG uptake and measured on each slice. When the lesion was extensively heterogeneous, the ROI was set so as to cover all of the components of the lesion. The maximum SUV measured on every scan was used for prognostic stratification.

Morphologic and Metabolic Response

MRI was used as a treatment monitoring method. MRI of the primary site was performed using a 1.5 Tesla system (Signa Horizon; GE Medical Systems, Milwaukee, WI, or Visart; Toshiba Medical Systems). Tumor size on MRI after the first cycle of neoadjuvant chemotherapy (t1) and after completion of neoadjuvant chemotherapy (t2) was compared with tumor size on the baseline study (t0). The percentage of size (t1 or t2) reduction rate was calculated by the formula: [Size (t1 or t2) − Size (t0)]/Size (t0) × 100%. Evaluation of metabolic response was accomplished by comparing the relative change in SUV and percent SUV (%SUV) reduction rate. The SUVs from PET/CT after the first cycle of neoadjuvant chemotherapy (t1) and after completion of neoadjuvant chemotherapy (t2) was compared with the SUVs on the baseline study (t0). The percentage SUV (t1 or t2) reduction rate was calculated by the following formula: [SUV (t1 or t2) − SUV (t0)]/SUV (t0) × 100%.

Histopathologic Response and Reference Standard

Histologic examinations were performed by an expert pathologist. Whenever necessary, immunohistochemical staining was carried out to confirm the diagnosis or tumor type according to the World Health Organization classification, TNM classification of the UICC for sarcoma of bone, and AJCC staging protocol for sarcoma of soft tissue.[33,34] In this study, the histologic grade of the tumors was determined using the grading system established by Hasegawa et al.[35–37] Histopathologic response to neoadjuvant chemotherapy was evaluated based on the grading system.[37–39] A favorable response to chemotherapy was defined as ≤10% viable tumor cells and an unfavorable response as >10% viable tumor cells. Two board-certified radiologists retrospectively reviewed the medical records and follow-up imaging studies. We evaluated follow-up imaging findings based on visual analysis as standard of reference. The designation of relapse was defined as local recurrence, nodal metastasis, or distant metastasis.

Statistical Analysis

The standard deviations (SD) of SUV (t1) and SUV (t2) are compared between metabolic responders and nonresponders as measures of heterogeneity by Student *t* test. The proportion of metabolic responders is compared based on histologic types by Kruskal-Wallis test. Overall survival (OS), which was from the time of baseline PET/CT study, for which the event was the first documentation of death, was chosen as the end point for assessment of prognostic value. Progression-free survival (PFS) was defined as the period between the time of the baseline PET/CT study and the occurrence of relapse or death, whichever came first. The Cox proportional-hazard model was applied to test the independence of established prognostic factors as outcome predictors. All P values calculated were 2-sided and adjusted for multiple testing. A $P < 0.05$ was considered indicative of statistical significance. Statistical analysis was performed with the PASW Statistics 18 software program (SPSS Inc, Chicago, IL).

RESULTS

The analyses were based on data obtained from 42 patients (Table 1). The most common anatomic site of the primary tumor was trunk (50%), followed by extremities (43%), and head and neck (7%). Of the tumors, 24% were less than 5-cm, 48% were in the 5- to 10-cm, and 28% were larger than 10-cm range. Pleomorphic sarcoma (n = 17, 40%) was the most common histologic subtype, followed by myxoid liposarcoma (n = 11, 26%), myxofibrosarcoma (n = 5, 12%), leiomyosarcoma (n = 3, 7%), dedifferentiated liposarcoma (n = 2, 5%), fibrosarcoma (n = 2, 5%), epithelioid sarcoma (n = 2, 5%), and alveolar soft part sarcoma (n = 1, 2%). The mean follow-up period of all 42 patients was 31 months (range, 5–52 months).

Distributions of SUV, tumor size, and reduction rate are summarized in Table 2. Baseline MRI showed tumors with a mean size (t0) ± SD of 77.5 ± 39.9 mm. After the first cycle (t1) and after completion (t2) of neoadjuvant chemotherapy, size was 65.6 ± 36.3 mm at (t1) and 54.1 ± 36.0 mm at (t2). The percent reduction rates

TABLE 1. Patient Characteristics

Characteristic	No. Patients
Age, yr	
Mean	54
SD	11
Range	32–72
Follow-up, mo	
Mean	31
SD	16
Range	5–52
Gender	
Male	26 (62)
Female	16 (38)
Size, cm	
0–5	10 (24)
5–10	20 (48)
>10	12 (28)
Distribution	
Trunk	24 (57)
Extremities	18 (43)

SD indicates standard deviation.

TABLE 2. Distributions of SUV, Tumor Size, and Reduction Rate

Baseline	
SUV (t0)	Size (t0), mm
10.9 ± 3.6 [3.8–19.6]	77.5 ± 39.9 [24.8–204.9]
Postneoadjuvant chemotherapy	
SUV (t1)	Size (t1), mm
7.8 ± 3.6 [1.9–13.8]	65.6 ± 36.3 [18.0–160.0]
SUV (t2)	Size (t2), mm
5.2 ± 3.4 [1.1–12.6]	54.1 ± 36.0 [5.0–155.0]
Reduction rate	
%SUV (t1) reduction rate	%Size (t1) reduction rate
28.8 ± 17.3 [2.0–78.0]	14.4 ± 20.0 [−18.2–72.7]
%SUV (t2) reduction rate	%Size (t2) reduction rate
51.7 ± 24.9 [2.0–94.0]	29.9 ± 26.4 [−18.2–92.9]

Data are presented as mean ± standard deviation (SD) with range.
SUV indicates standardized uptake value; t0, baseline; t1, after the first cycle; t2, after completion of neoadjuvant chemotherapy.

of size (t1) and size (t2) were 14.4 ± 20.0% at (t1) and 29.9 ± 26.4% at (t2). Baseline PET/CT showed high FDG uptake with a mean SUV (t0) ± SD of 10.9 ± 3.6. After the first cycle of neoadjuvant chemotherapy, the SUV had decreased to 7.8 ± 3.4, and then it had decreased further to 5.2 ± 3.4 after completion of neoadjuvant chemotherapy (Table 2). The SDs of SUV (t1) and SUV (t2) compared between metabolic responders and nonresponders as measures of heterogeneity showed that no significant difference was found in SUV (t1) (metabolic responder vs. nonresponder, 3.0 vs. 2.9, $P = 0.534$) and SUV (t2) (metabolic responder vs. nonresponder, 2.9 vs. 2.5, $P = 0.711$). The proportion of metabolic responders compared on the basis of histologic types revealed that there was no significant difference in %SUV (t1) reduction rate ($P = 0.545$) and %SUV (t2) reduction rate ($P = 0.671$) (Table 3). By using a previously defined threshold of 35% decrease in SUV, 15 of the 42 patients (36%) were classified as

TABLE 3. Metabolic Responder and Nonresponders by Histologic Type

	%SUV (t1) Reduction Rate		%SUV (t2) Reduction Rate	
	Metabolic Nonresponder	Metabolic Responder	Metabolic Nonresponder	Metabolic Responder
MFH	12 (29)	5 (12)	8 (19)	9 (21)
MLS	7 (17)	4 (10)	4 (10)	7 (17)
LMS	3 (7)	0	2 (5)	1 (2)
MFS	2 (5)	3 (7)	1 (2)	4 (10)
FS	1 (2)	1 (2)	1 (2)	1 (2)
ASPS	1 (2)	0	0	1 (2)
DDL	1 (2)	1 (2)	0	2 (5)
ES	0	1 (2)	0	1 (2)

The numbers of parentheses are percentages.
The proportion of metabolic responders do not depend on histologic types with %SUV (t1) reduction rate ($P = 0.545$) and %SUV (t2) reduction rate ($P = 0.671$) by Kruskal-Wall test.
MFH indicates malignant fibrous histiocytoma; MLS, myxoid liposarcoma; LMS, leiomyosarcoma; FS, fibrosarcoma; ASPS, alveolar soft part sarcoma; DDL, dedifferentiated liposarcoma; ES, epithelioid sarcoma.

metabolic responders with a mean ± SD %SUV (t1) reduction rate of 43.8 ± 18.0% and the other 27 patients (64%) were classified as metabolic nonresponders who had a mean ± SD %SUV (t1) reduction rate of 20.5% ± 9.6% after the first cycle of neoadjuvant chemotherapy. After completion of neoadjuvant chemotherapy, 26 of the 42 patients (62%) were classified as metabolic responders with a mean ± SD %SUV (t2) reduction rate of 63.9% ± 18.6%. Sixteen patients (38%) were classified as metabolic nonresponders who had a mean ± SD %SUV (t2) reduction rate of 28.6% ± 14.3%. The correlation between %SUV (t1) reduction rate and %size (t1) reduction rate, and between %SUV (t2) reduction rate and %size (t2) reduction rate were not significant (t1: $r = -0.092$, $P = 0.561$; t2: $r = 0.304$, $P = 0.050$).

Therapeutic response evaluated by histopathology resulted in 10 patients (24%) with satisfactory response and 32 patients (76%) with unsatisfactory response after completion of neoadjuvant chemotherapy (Fig. 1). The SUV (t1) and SUV (t2) of the histopathologic nonresponders were significantly higher as compared with those of the histopathologic responders ($P = 0.007$ and $P = 0.033$, respectively). However, no significant associations were found between the histopathologic response and size (t0), size (t1), size (t2), and SUV (t0). Metabolic responders defined as having at least 35% decrease in %SUV reduction rate showed more frequent histopathologic response compared with metabolic nonresponders ($P = 0.009$ for %SUV (t1) reduction rate and $P = 0.004$ for %SUV (t2) reduction rate, respectively), whereas there were no associations between histopathologic response and %size reduction rate. The sensitivity, specificity, positive predictive value, negative predictive value, and accuracy of %SUV reduction rate for favorable histologic response were 46.7%, 88.9%, 70.0%, 75.0%, and 73.8% for %SUV (t1) reduction rate, respectively, and 38.5%, 100%, 100%, 50.0%, and 61.9% for %SUV (t2) reduction rate, respectively. No significant association was found between histologic response and %size reduction rate. Fourteen of the 42 patients (33%) have developed recurrence, with a mean time to recurrence of 9.0 months. The 2-year and 4-year actuarial PFS rates were 68.6% and 27.1%, respectively. Univariate analyses of potential prognostic factors demonstrated that PFS was associated with histopathologic response, SUV (t2), %SUV (t1) reduction rate, and %SUV (t2) reduction rate (Fig. 2, Table 4). Age, glucose transporter protein 1,

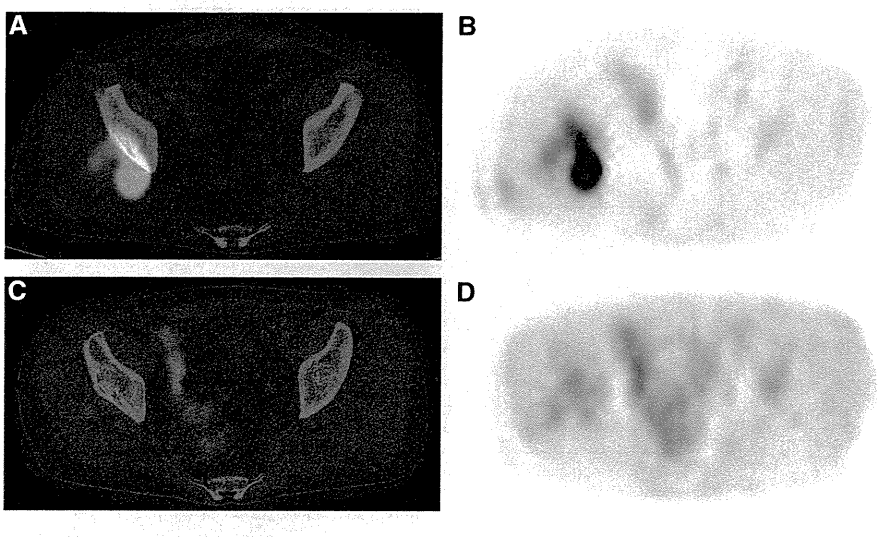

FIGURE 1. Responder of neoadjuvant chemotherapy. (**A, B**) Transaxial F-18 FDG PET/CT images demonstrate significant uptake in the tumor of the right buttock which is pathologically confirmed as pleomorphic sarcoma. (**C, D**) Transaxial F-18 FDG PET/CT images demonstrate metabolic reduction in the tumor of the right buttock after neoadjuvant chemotherapy.

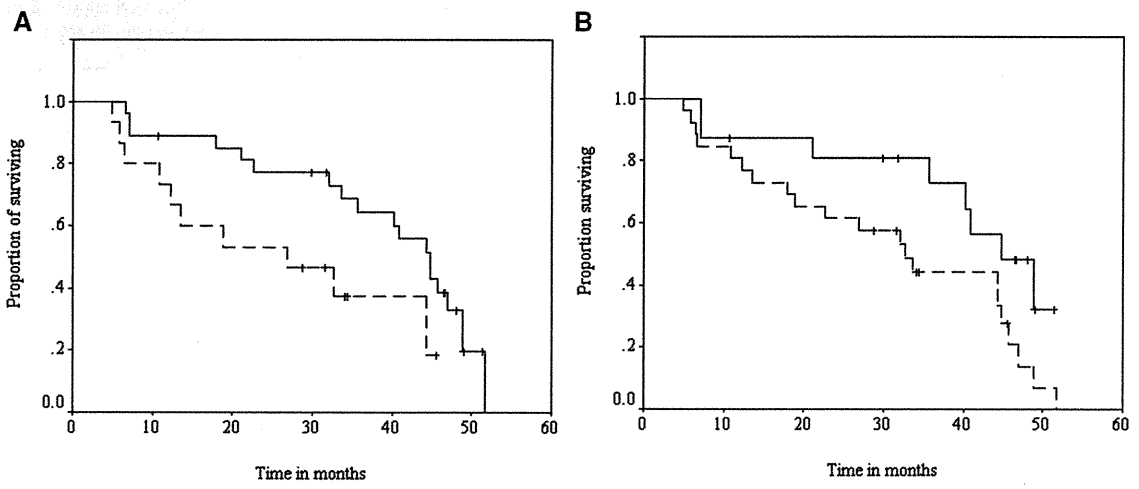

FIGURE 2. A, The PFS of %SUV (t1) reduction rate after the first cycle of neoadjuvant chemotherapy. Solid line: %SUV (t1) reduction rate is ≥30%. Dash line: %SUV (t1) reduction rate is less than 30%. **B,** The PFS of %SUV (t2) reduction rate after completion of neoadjuvant chemotherapy. Solid line: %SUV (t2) reduction rate is ≥60%. Dash line: %SUV (t2) reduction rate is less than 60%.

size (t0, t1, t2), SUV (t0, t1, t2), and %size (t1, t2) reduction rate failed to show a predictive value. A multivariate analysis of factors related to disease progression was performed. In order of relative risk, histopathologic response and %SUV (t2) reduction rate were independent predictors of PFS (Table 4). The SUV (t2) and %SUV (t1) reduction rate were not found to be identical order of relative risk.

The OS for the 42 patients was 83.3% at 2 years and 32.9% at 4 years. Univariate analyses showed that OS had a significant association with histopathologic response, %SUV (t1) reduction rate, and %SUV (t2) reduction rate (Fig. 3, Table 4). However, size (t0, t1, t2), SUV (t0, t1, t2), and %size (t1, t2) reduction rate failed to show a predictive value. In the multivariate analysis, histopathologic response and %SUV (t2) reduction rate showed strong independent value for the prediction of OS (Table 5). The %SUV (t1) reduction rate failed to show independent prognostic properties.

DISCUSSION

In this study, we examined the therapeutic effect and prognostic value of F-18 FDG PET/CT after neoadjuvant chemotherapy in patients with high-grade sarcoma. We found that the histopathologic response and metabolic reduction rate had significant association with PFS and OS. Tumors of histopathologic responders showed high metabolic reduction, which was similar to the results of recent studies.[40]

The prognostic importance of metabolic reduction after neoadjuvant chemotherapy has been suggested in the literature.[22–30] In clinical setting for patients with soft-tissue sarcomas of the extremities, metabolic reduction in F-18 FDG uptake after neoadjuvant chemotherapy was at high risk of systemic disease recurrence.[41] In a study of 36 patients with Ewing sarcoma family tumors, neoadjuvant chemotherapy-induced metabolic reduction after 3 to 7 cycles was noted and SUV after neoadjuvant chemotherapy <2.5 was predictive of PFS.[40] Furthermore, a change in the size of the tumor after neoadjuvant chemotherapy is frequently used in clinical practice to evaluate therapeutic response in patients with high-grade sarcoma. The size reduction evaluated by standard CT has not been correlated consistently with histologic response or with outcome.[6–8] This may relate to the limited availability of this diagnostic modality. In contrast, PET or PET/CT allows semi-quantitative assessment of uptake that is convenient to evaluate tumor viability during

TABLE 4. Univariate Analyses of PFS and OS

Characteristic	No. Patients	2-yr PFS (%)	4-yr PFS (%)	*P*	2-yr OS (%)	4-yr OS (%)	*P*
Age, yr							
≥56	22	59	12	0.181	74	20	0.234
<56	20	74	43		94	51	
Histologic response							
Nonresponder	32	58	12	0.0004	81	16	0.0007
Responder	10	90	75		90	77	
Glut-1 expression							
Positive	25	68	28	0.539	86	27	0.596
Negative	17	64	33		80	41	
Size (t0), mm							
≥72	21	66	20	0.58	78	28	0.52
<72	21	66	32		89	40	
Size (t1), mm							
≥56	22	63	19	0.45	84	28	0.59
<56	20	69	33		83	40	
Size (t2), mm							
≥45	23	65	30	0.89	85	40	0.95
<45	19	68	20		82	24	
%Size (t1) reduction rate							
≥6.2	21	71	34	0.164	84	45	0.122
<6.2	21	61	18		83	23	
%Size (t2) reduction rate							
≥29.5	21	76	30	0.19	94	38	0.128
<29.5	21	56	22		72	29	
SUV (t0)							
≥11.7	22	71	24	0.7	90	28	0.88
<11.7	20	60	29		73	39	
SUV (t1)							
≥6.6	20	68	25	0.96	84	31	0.91
<6.6	22	63	29		83	38	
SUV (t2)							
≥3.9	21	51	8	0.007	81	13	0.14
<3.9	21	81	40		86	43	
%SUV (t1) reduction rate							
≥30	15	92	69	0.0012	92	71	0.005
<30	27	56	9		75	13	
%SUV (t2) reduction rate							
≥60	26	96	40	<0.0001	96	43	0.0001
<60	16	26	0		51	0	

PFS indicates progression-free survival; OS, overall survival; Glut-1, glucose transporter protein-1; t0, baseline; t1, after the first cycle; t2, after completion of neoadjuvant chemotherapy.

therapy. Moreover, good correlations have been demonstrated between histologic response and changes in F-18 FDG accumulation after neoadjuvant chemotherapy in patients with various histologic kinds of tumors.[22–30] Tumor response determined by reduction of F-18 FDG uptake after neoadjuvant chemotherapy was found to be an early indicator of improved PFS or OS.[26–30] Our data demonstrate that significant metabolic reduction after neoadjuvant chemotherapy evaluated by PET/CT has a possibility to portend a favorable outcome and provides compelling support for the routine use of this technique in patients with high-grade sarcoma.

We demonstrate possible correlations of measures of fall in SUV after the first cycle and completion of neoadjuvant chemotherapy and survival. A decrease in SUV after neoadjuvant chemotherapy with median cutoff value of 30% or 60% has been used. The use of change in %SUV reduction rate after the first cycle and after completion of induction chemotherapy as a continuous variable confirmed the predictive ability of metabolic reduction to predict less favorable outcome. A prior study revealed that the ratio of pre- and postchemotherapeutic SUV was correlated with histologic response in patients with high-grade sarcoma.[20] Our data provide a support for this, as patients experiencing such a level of metabolic reduction exhibited favorable PFS and OS, although with a short follow-up duration and a wide confidence interval.

Treatment-induced pathologic necrosis has been demonstrated to be an independent predictor of outcome in patients who have received neoadjuvant chemotherapy for high-grade soft-tissue sarcoma.[1–5] Evaluation of pathologic specimens is warranted to perform precise assessment of response to neoadjuvant chemotherapy. In the prior studies using PET or PET/CT, metabolic reduction after neoadjuvant chemotherapy is capable of reflecting histopathologic response.[42–47] A decrease in SUV after neoadjuvant chemotherapy correlates with the percent of pathologic necrosis. However, such a correlation has been suggested, as yet there has been no studies assessing the direct association between metabolic reduction, histopathologic response, and outcome. In an attempt to resolve this issue in the present study, we investigated whether metabolic response could reflect histopathologic response and could have association with PFS or OS. Our data demonstrated that metabolic reduction after neoadjuvant chemotherapy showed significant correlation with histopathologic response and had a possibility to reflect favorable outcome.

The prognostic value of SUV likely reflects the cumulative effect of a maximum value of different ROIs within the heterogeneous tumor. The results of the previous study revealed a fair association between measures of preoperative SUV and poor outcome.[13] The other study documented that mean SUV on the preoperative PET images of patients with resectable soft-tissue sarcoma predicted outcome.[15] Given the prognostic value of postchemotherapeutic SUV in patients with Ewing sarcoma in a retrospective study,[47] a measurement of SUV after neoadjuvant chemotherapy in high-grade sarcoma may reflect in vivo chemotherapeutic sensitivity. The probable ability of SUV measurements to assess complicated metabolic interactions and predicting outcome makes %SUV reduction rate an important tool for management of patients with high-grade sarcoma. Further prospective studies should confirm whether %SUV reduction rate may be an independent prognostic factor.

Another novel finding in the present study is the documentation that a decrease in SUV after neoadjuvant chemotherapy is a common phenomenon in patients with high-grade sarcoma. Although most of the studies evaluating metabolic reduction have relied on 2-point PET studies at baseline and after neoadjuvant chemotherapy, several studies have assessed metabolic reduction based on sequential PET scans during neoadjuvant chemotherapy in patients with solid tumors.[48,49] Metabolic reduction after the first and third cycle of neoadjuvant chemotherapy was found to be correlated significantly with OS in patients with ovarian cancer.[48] Similarly, in a study of 11 patients with breast cancer, metabolic reduction after the first and second cycles of neoadjuvant chemotherapy was 28% and 46% in the responding lesions, respectively.[49] Because chemotherapeutic response depends on the therapeutic regimens and histologic type of tumor, the degree of

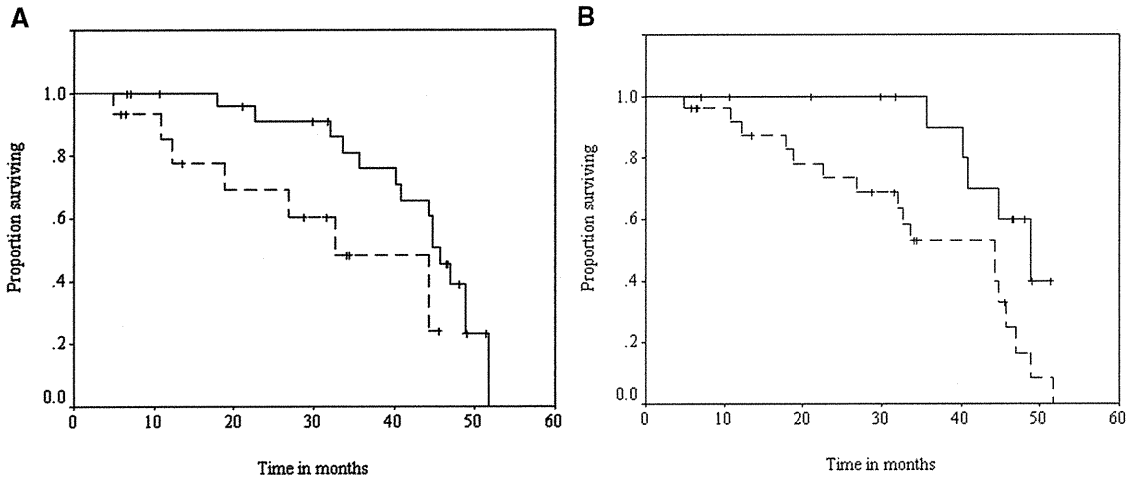

FIGURE 3. A, The OS of %SUV (t1) reduction rate after the first cycle of neoadjuvant chemotherapy. Solid line: %SUV (t1) reduction rate is ≥30%. Dash line: %SUV (t1) reduction rate is less than 30%. **B,** The OS of %SUV (t2) reduction rate after completion of neoadjuvant chemotherapy. Solid line: %SUV (t2) reduction rate is ≥60%. Dash line: %SUV (t2) reduction rate is less than 60%.

TABLE 5. Multivariate Analyses of PFS and OS

Characteristic	B	Wald	HR	LCI	HCI	*P*
PFS						
Histopathologic response	2.00	6.67	7.35	1.62	33.40	0.01
%SUV (t2) reduction rate	2.00	7.99	7.32	1.84	29.10	0.005
OS						
Histopathologic response	1.92	6.14	6.80	1.49	30.94	0.013
%SUV (t2) reduction rate	2.33	13.61	10.31	2.99	35.64	<0.0001

PFS indicates progression-free survival; OS, overall survival; B, regression coefficient; LCI, lower confidence interval; HCI, higher confidence interval; HR, hazard ratio.

metabolic reduction may be different after every cycle of chemotherapy. Importantly, our study examines patients with specific histologic diagnoses and confirms that metabolic reduction after induction chemotherapy is a common finding in patients with high-grade sarcoma.

The limitations of the present study included the small number of patients and relatively short duration of follow-up period. The diversity of histologic diagnoses had a potential of bias, but the proportion of metabolic responder and nonresponder based on each histologic subtype was not statistically significant. This study focused on patients with high-grade sarcoma who underwent neoadjuvant chemotherapy and the data cannot be extrapolated to patients with advanced stage. A validation study using sequential PET/CT scans is needed in a larger population with various histologic types and adequate follow-up period. The cost-effectiveness of sequential PET/CT for predicting the therapeutic efficacy after neoadjuvant chemotherapy needs to be considered. The role of sequential PET/CT in reducing the number of ineffective chemotherapies in nonresponders must be clarified.

In conclusion, our data also suggest that metabolic reduction after neoadjuvant chemotherapy evaluated using PET/CT can be used for stratification of patients with high-grade sarcoma in clinical trials, as 2 groups of responders and nonresponders exhibit a very different survival profile. Further research is required to determine the role of serial measures of PET/CT in the long-term follow-up period and whether metabolic reductions evaluated by PET/CT can be used as a surrogate for outcome.

REFERENCES

1. Tierney JF; Sarcoma Meta-analysis Collaboration. Adjuvant chemotherapy for localized resectable soft-tissue sarcoma of adults: meta-analysis of individual data. *Lancet.* 1997;350:1647–1654.
2. Yang JC, Chang AE, Baker AR, et al. Randomized prospective study of the benefit of adjuvant radiation therapy in the treatment of soft tissue sarcomas of the extremity. *J Clin Oncol.* 1998;16:197–203.
3. Frustaci S, Gherlinzoni F, de Paoli A, et al. Adjuvant chemotherapy for adult soft tissue sarcomas of the extremities and girdles: results of the Italian randomized cooperative trial. *J Clin Oncol.* 2001;19:1238–1247.
4. Pezzi CM, Pollock RE, Evans HL, et al. Preoperative chemotherapy for soft-tissue sarcomas of the extremities. *Ann Surg.* 1990;211:476–481.
5. Pisters PW, Patel SR, Verma DG, et al. Preoperative chemotherapy for stage IIIB extremity soft tissue sarcoma: long-term results from a single institution. *J Clin Oncol.* 1997;15:3481–3487.
6. Wendtner CM, Abdel-Rahman S, Krych M, et al. Response to neoadjuvant chemotherapy combined with regional hyperthermia predicts long-term survival for adult patients with retroperitoneal and visceral high-risk soft tissue sarcomas. *J Clin Oncol.* 2002;20:3156–3164.
7. Meric F, Hess KR, Verma DG, et al. Radiographic response to neoadjuvant chemotherapy is predictor of local control and survival in soft tissue sarcomas. *Cancer.* 2002;95:1120–1126.
8. Delaney TF, Spiro IJ, Suit HD, et al. Neoadjuvant chemotherapy and radiotherapy for large extremity soft-tissue sarcomas. *Int J Radiat Oncol Biol Phys.* 2003;56:1117–1127.
9. Nieweg OE, Prium J, van Ginkel RJ, et al. Fluorine-18 fluorodeoxyglucose PET imaging of soft-tissue sarcoma. *J Nucl Med.* 1996;37:257–261.
10. Schwarzbach MHM, Dimitrakopoulou-Strauss A, Willeke F, et al. Clinical value of [18-F] fluorodeoxyglucose positron emission tomography imaging in soft tissue sarcomas. *Ann Surg.* 2000;231:380–386.
11. Eary JF, Conrad EU, Bruckner JD, et al. Quantitative [F-18]fluorodeoxyglucose positron emission tomography in pretreatment and grading of sarcoma. *Clin Cancer Res.* 1998;4:1214–1220.
12. Ioannidis JP, Lau J. ^{18}F-FDG PET for the diagnosis of soft tissue sarcoma: a meta-analysis. *J Nucl Med.* 2003;44:717–724.
13. Folpe AL, Lyles RH, Sprouse JT, et al. (F-18) fluorodeoxyglucose positron emission tomography as a predictor of pathologic grade and other prognostic variables in bone and soft tissue sarcoma. *Clin Cancer Res.* 2000;6:1279–1287.
14. Eary JF, O'Sullivan F, Powitan Y, et al. Sarcoma tumor FDG uptake measured by PET and patient outcome: a retrospective analysis. *Eur J Nucl Med.* 2002;29:1149–1154.

15. Schwarzbach MHM, Hinz U, Dimitrakopoulou-Strauss A, et al. Prognostic significance of preoperative [18-F]fluorodeoxyglucose (FDG) positron emission tomography (PET) imaging in patients with resectable soft tissue sarcomas. *Ann Surg.* 2005;241:286–294.
16. Tateishi U, Yamaguchi U, Seki K, et al. Glut-1 expression and enhanced glucose metabolism are associated with tumor grade in bone and soft tissue sarcomas: a prospective evaluation by [18F]fluorodeoxyglucose positron emission tomography. *Eur J Nucl Med Mol Imaging.* 2006;33:683–691.
17. Ito S, Nemoto T, Satoh S, et al. Human rhabdomyosarcoma cells retain insulin-regulated glucose transport activity through glucose transporter 1. *Arch Biochem Biophys.* 2000;3:72–82.
18. Eary JF, Mankoff DA. Tumor metabolic rates in sarcoma using FDG PET. *J Nucl Med.* 1998;39:250–254.
19. Lowe VJ, Dunphy FR, Varvares M, et al. Evaluation of chemotherapy response in patients with advanced head and neck cancer using [F-18]fluorodeoxyglucose positron emission tomography. *Head Neck.* 1997;19:666–674.
20. Smith C, Welch AE, Hutcheon AW, et al. Positron emission tomography using [(18)F]-fluorodeoxy-D-glucose to predict the pathologic response of breast cancer to primary chemotherapy. *J Clin Oncol.* 2000;18:1676–1688.
21. Schelling M, Avril N, Nahrig J, et al. Positron emission tomography using [(18)F]fluorodeoxyglucose for monitoring primary chemotherapy in breast cancer. *J Clin Oncol.* 2000;18:1689–1695.
22. Weber WA, Ott K, Becker K, et al. Prediction of response to preoperative chemotherapy in adenocarcinomas of the esophagogastric junction by metabolic imaging. *J Clin Oncol.* 2001;19:3058–3065.
23. Ott K, Fink U, Becker K, et al. Prediction of response to preoperative chemotherapy in gastric carcinoma by metabolic imaging: results of a prospective trial. *J Clin Oncol.* 2003;21:4604–4610.
24. Stoobants S, Goeminne J, Seegers M, et al. 18FDG-Positron emission tomography for the early prediction of response in advanced soft tissue sarcoma treated with imatinib mesylate (Glivec). *Eur J Cancer.* 2003;39:2012–2020.
25. Downy R, Akhurst T, Ilson D, et al. Whole body ^{18}FDG-PET and the response of esophageal cancer to induction therapy: results of a prospective trial. *J Clin Oncol.* 2003;21:428–432.
26. Hutchings M, Mikhaeel NG, Fields PA, et al. Prognostic value of interim FDG-PET after two or three cycles of chemotherapy in Hodgkin lymphoma. *Ann Oncol.* 2005;16:1160–1168.
27. Mikhaeel NG, Hutchings M, Fields PA, et al. FDG-PET after two to three cycles of chemotherapy predicts progression-free and overall survival in high-grade non-Hodgkin lymphoma. *Ann Oncol.* 2005;16:1514–1523.
28. Haioun C, Itti E, Rahmouni A, et al. [^{18}F]fluoro-2-deoxy-D-glucose positron emission tomography (FDG-PET) in aggressive lymphoma: an early prognostic tool for predicting patient outcome. *Blood.* 2005;106:1376–1381.
29. Hutchings M, Loft A, Hansen M, et al. FDG-PET after two cycles of chemotherapy predicts treatment failure and progression-free survival in Hodgkin lymphoma. *Blood.* 2006;107:52–59.
30. Pöttgen C, Levegrün S, Theegarten D, et al. Value of ^{18}F-fluoro-2-deoxy-D-Glucose-Positron emission tomography/computed tomography in non-small-cell lung cancer for prediction of pathologic response and times to relapse after neoadjuvant chemoradiotherapy. *Clin Cancer Res.* 2006;12:97–106.
31. Benz RM, Czernin J, Allen-Auerbach MS, et al. FDG-PET/CT imaging predicts histopathologic treatment responses and after the initial cycle of neoadjuvant chemotherapy in high-grade soft-tissue sarcomas. *Clin Cancer Res.* 2009;15:2856–2863.
32. Oken MM, Creech RH, Tormey DC, et al. Toxicity and response criteria of the Eastern Cooperative Oncology Group. *Am J Clin Oncol.* 1982;5:649–655.
33. Sobin LH, Wittekind C; International Union Against Cancer (UICC): *TNM Classification of Malignant Tumours.* 6th ed. New York, NY: Wiley; 2002.
34. Green FL, Page DL, Fleming ID, et al. *AJCC Cancer Staging Manual.* 6th ed. New York, NY: Springer; 2002.
35. Fletcher CDM, Unni KK, Mertens F. *World Health Organization Classification of Tumours. Pathology and Genetics of Tumours of Soft Tissue and Bone.* Lyon, France: IARC Press; 2002.
36. Hasegawa T, Yamamoto S, Yokoyama R, et al. Prognostic significance of grading and staging system using MIB-1 score in adult patients with soft tissue sarcoma of the extremities and trunk. *Cancer.* 2002;95:843–851.
37. Hasegawa T, Yamamoto S, Nojima T, et al. Validity and reproducibility of histologic diagnosis and grading for adult soft-tissue sarcomas. *Hum Pathol.* 2002;33:111–115.
38. Salzer-Kuntschik M, Delling G, Beron G, et al. Morphological grades of regression in osteosarcoma. *J Cancer Res Clin Oncol.* 1983;106:21–24.
39. Jürgens H, Exner U, Gadner H, et al. Multidisciplinary treatment of Ewing's sarcoma of bone: a 6-year experience of a European cooperative group. *Cancer.* 1988;61:23–32.
40. Evilevitch V, Weber WA, Tap WD, et al. Reduction of glucose metabolic activity is more accurate than change in size at predicting histopathologic response to neoadjuvant therapy in high-grade soft-tissue sarcomas. *Clin Cancer Res.* 2008;14:715–720.
41. Eisenhauer EA, Therasse P, Bogaerts J, et al. New response evaluation criteria in solid tumours: revised RECIST guideline (version 1. 1). *Eur J Cancer.* 2009;45:228–247.
42. Jones DN, McCowage GB, Sostman HD, et al. Monitoring of neoadjuvant therapy response of soft-tissue and musculoskeletal sarcoma using fluorine-18-FDG PET. *J Nucl Med.* 1996;37:1438–1444.
43. Schulte M, Brecht-Krauss D, Werner M, et al. Evaluation of neoadjuvant therapy response of osteogenic sarcoma using FDG PET. *J Nucl Med.* 1999;40:1637–1643.
44. Vernon CB, Eary JF, Rubin BP, et al. FDG PET imaging guided re-evaluation of histopathologic response in a patient with high-grade sarcoma. *Skeletal Radiol.* 2003;32:139–142.
45. Iagaru A, Masamed R, Chawla SP, et al. F-18 FDG PET and PET/CT evaluation of response to chemotherapy in bone and soft tissue sarcomas. *Clin Nucl Med.* 2008;33:8–13.
46. Piperkova E, Mikhaeil M, Mousavi A, et al. Impact of PET and CT in PET/CT studies for staging and evaluating treatment response in bone and soft tissue sarcomas. *Clin Nucl Med.* 2009;34:146–150.
47. Hawkins DS, Schuetze SM, Butrynski JE, et al. [^{18}F]fluorodeoxyglucose positron emission tomography predicts outcome for Ewing sarcoma family of tumors. *J Clin Oncol.* 2005;23:8828–8834.
48. Avril N, Sassen S, Schmalfeldt B, et al. Prediction of response to neoadjuvant chemotherapy by sequential F-18-fluorodeoxyglucose positron emission tomography in patients with advanced-stage ovarian cancer. *J Clin Oncol.* 2005;23:7445–7453.
49. Dose Schwarz J, Bader M, Jenicke L, et al. Early prediction of response to chemotherapy in metastatic breast cancer using sequential 18F-FDG PET. *J Nucl Med.* 2005;46:1144–1150.

Brain Tumor Pathol (2011) 28:43–51
DOI 10.1007/s10014-010-0002-4

ORIGINAL ARTICLE

Precise comparison of protoporphyrin IX fluorescence spectra with pathological results for brain tumor tissue identification

Takehiro Ando · Etsuko Kobayashi · Hongen Liao · Takashi Maruyama · Yoshihiro Muragaki · Hiroshi Iseki · Osami Kubo · Ichiro Sakuma

Received: 3 March 2010 / Accepted: 13 July 2010 / Published online: 25 December 2010

Abstract Photodynamic diagnosis is used during glioma surgery. Although some studies have shown that the spectrum of fluorescence was efficient for precise tumor diagnosis, previous methods to characterize the spectrum have been problematic, which can lead to misdiagnosis. In this paper, we introduce a comparison technique to characterize spectrum from pathology and results of preliminary measurement using human brain tissues. We developed a spectrum scanning system that enables spectra measurement of raw tissues. Because tissue preparations retain the shape of the device holder, spectra can be compared precisely with pathological examination. As a preliminary analysis, we measured 13 sample tissues from five patients with brain tumors. The technique enabled us to measure spectra and compare them with pathological results. Some tissues exhibited a good relationship between spectra and pathological results. Although there were some false positive and false negative cases, false positive tissue had different spectra in which intensity of short-wavelength side was also high. The proposed technique provides an accurate comparison of quantitative fluorescence spectra with pathological results. We found that spectrum analysis may reduce false positive errors. These results will increase the accuracy of tumor tissue identification.

Keywords 5-Aminolevulinic acid · Protoporphyrin IX · Fluorescence spectra · Photodynamic diagnosis

T. Ando (✉) · E. Kobayashi · H. Liao · I. Sakuma
Department of Bioengineering, Graduate School of Engineering, The University of Tokyo, Engineering building No.14, Room 722, Hongo 7-3-1, Bunkyo, Tokyo 113-8656, Japan
e-mail: take_and_o@bmpe.t.u-tokyo.ac.jp

T. Maruyama · H. Iseki · O. Kubo
Department of Neurosurgery, Neurological Institute, Tokyo Women's Medical University, Shinjuku, Tokyo 162-8666, Japan

Y. Muragaki · H. Iseki
Institute of Advanced Biomedical Engineering and Science, Tokyo Women's Medical University, Shinjuku, Tokyo 162-8666, Japan

Introduction

Over recent decades, photodynamic diagnosis (PDD) has been studied for intraoperative tumor diagnosis, especially glioma. PDD uses autofluorescence or endogenous fluorescence materials [1–4], and the technique can be easily applied for clinical practice because the system is simple. In a number of clinical studies, 5-aminolevulinic acid (5-ALA)-induced protoporphyrin IX (PpIX) fluorescence has been used for intraoperative tumor diagnosis. Although 5-ALA and PpIX are natural substances produced by the human body, orally administrated 5-ALA accumulates in tumor cells and is converted to PpIX by heme biosynthesis. Accumulation of 5-ALA in a tumor cell may be caused by a damaged blood brain barrier (BBB) or iron (Fe)-metabolic enzyme defect, such as ferrochelatase [5]. However, the exact mechanism is still unknown.

Stummer et al. [1–3] introduced the use of the fluorescence surgical microscope to examine PpIX fluorescence for intraoperative tumor detection. They reported that some regions of brain and tumor tissue have different fluorescence characteristics (intensity and color) and assessed these tissues pathologically. Although this approach was appropriate for fluorescence-guided surgery, fluorescence measurement was not quantitative. A recent study of quantitative fluorescence measurement showed that PpIX spectrum shape is important to precisely detect tumor and

diagnose malignancy [6]. Another group reported that ultraviolet (UV) laser and white light reveal differences in the autofluorescence spectra between tumor and normal brain tissue [7, 8]. Although these quantitative studies found characteristic tumor tissue spectra when comparing them with pathological results, the comparison methods used have the following limitations. First, there is a possibility that a spectrum measurement point is different from a pathology examination point. This means that a spectrum characterization may not be correct. Second, because the spectrum measurement was performed after staining or fixation with formalin, the measured spectrum may be different from that of the raw tissue. To use the result in situ, raw tissue spectrum measurement is necessary. Finally, although tumor margin characterization is necessary for precise resection, these methods cannot determine spatial changes in spectra.

To solve these problems, we developed a spectrum scanning system that enables acquisition of raw tissue spectra distribution. Furthermore, our novel protocol makes it possible to precisely compare spectra with pathological results. In this paper, we introduce the technique we devised and present results of preliminary measurements.

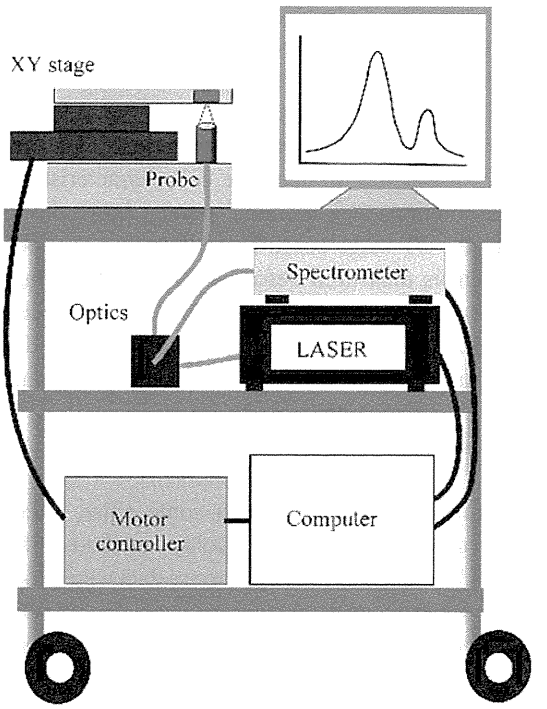

Fig. 1 Overall view of the measurement system

Materials and methods

Measurement system

A spectrum-scanning system for 5-ALA-induced PpIX fluorescence was especially designed for both fluorescence measurement and fluorescence spectra comparison with pathological results. The system consists of an excitation laser (VLS405-SA3, Digital Stream), a spectrometer (WTC-111E B&W, TEK Inc.), optics, and a computer (Fig. 1). The excitation laser emits 405 nm of UV light, and the maximal output power is 15 mW. The spectrometer wavelength range is 300–850 nm. The measurement probe uses a coaxial optical system. All light paths are connected with optical fibers (core diameter 365 μm, multimode), and a dichroic mirror is used to separate excitation light and fluorescence. To insert a dichroic mirror in the light path, three collimator lenses are mounted to a cubic box. Angles and positions of all collimator lenses and the dichroic mirror angle can be adjusted to improve the coupling efficiency of the light. It is also equipped with a long-pass filter to separate strong reflected excitation light from the fluorescence signal. There are two achromatic lenses at the tip of the probe. The focal length of the fiber side lens is 19 mm, the object side is 30 mm, the working distance is 21.7 mm, and the lens diameter is 12.5 mm. The measurement spot diameter is evaluated using a phantom, the optical character of which is designed to match that of brain tissue. As a result, the system's measuring diameter is estimated as 0.8 mm.

To measure fluorescence spectra spatial changes, the measurement probe is fixed under an *XY* stage (SGSP20-35XY, Sigma Koki), and the sample tissues are then moved. A removable tissue holder that has a square 5-mm hole is set on the stage. One corner of the holder hole is cut down to make a shape mark. Because the holder location is registered to the *XY* stage coordinates, it is possible to follow the measuring position. In this study, spectra of 58 points were acquired from each sample tissue.

Measurement protocol

To accurately compare spectra with pathological results, we devised the following measurement protocol:

1. Resected tissue was gently put in the measurement system tissue holder.
2. The spectrum of each point was measured by the system, and data were processed automatically.
3. After measurement, the tissue and the holder were put in liquid nitrogen to freeze the tissue.
4. The frozen tissue was taken out of the holder and sectioned using conventional methods.
5. The sectioned tissue was stained with hematoxylin–eosin (H&E).

Sectioning and staining were performed by a pathologist. Spectrometer exposure time and the laser power were

arbitrarily adjusted depending on each patient. Although this protocol is relatively complicated, because the frozen tissue retains the original shape of the holder and the measured surface can be maintained, it is possible to make a "holder-shaped" histological preparation. This preparation makes it possible to compare cell characteristics with the corresponding measurement points from the tissue shape and the *XY*-stage coordinates. Furthermore, because the spectrum is measured before freezing or staining, this method allows the use of raw brain tissue spectra for comparison. This means that the results can be directly applied to intraoperative measurement and resection.

Data processing

Because measured spectra contain some noise, data were smoothed using the Savitzky–Golay method (25-point smoothing) [9]. After smoothing, spectra data were processed to extract each PpIX peak intensity and wavelength from raw data, which contain autofluorescence spectra. The procedure is as follows: First, we empirically approximated a curve of a background autofluorescence spectrum as a quartic function using the least mean squares (LMS) method. To draw the LMS curve, data sets of 590–610 and 747–913 nm were used (Fig. 2). After LMS curve (background) subtraction from raw data, PpIX peak intensity and wavelength were calculated as maximal intensity and its wavelength. We recorded not only the PpIX intensity but also intensity at 585 nm, which represents the intensity of short-wavelength side. These data were plotted on a contour map.

Ex vivo measurement and pathological examination

Using the system we developed, we measured brain tissues resected during brain tumor operations at Tokyo Women's Medical University Hospital. At 7:30 a.m. on the day of the operation, 5-ALA at a dosage of 20 mg/kg body weight was orally administered to patients who were suspected of having a glioma. We targeted primary gliomas in five patients whose magnetic resonance image MRI results suggested that the tumors were grade III or IV. Measurement was performed at about 2:00 p.m. on the same day. Preparations for pathological examinations were made using the method mentioned earlier. Spectrometer exposure time was arbitrary set to 70–500 ms for each measurement point. Measurement time, including processing time, was approximately 10–40 s for each sample tissue. The pathological examinations were performed by a pathologist, and examiners were blinded to fluorescence measurement. All experimental protocols were approved by the Ethical Committee of Tokyo Women's Medical University.

Results

Tumor types of each patient in this study were as follows:

Case 1: Glioblastoma multiforme (GBM)
Case 2: Anaplastic oligodendro-astrocytoma (AOA)
Case 3: Anaplastic oligodendroglioma (AO)
Case 4: Oligodendroglioma (O)
Case 5: GBM

We obtained one tissue from case 1, four from case 2, three from case 3, one from case 4, and four from case 5. Each tissue is represented by a number (case number) and alphabetic letters. Figures 3–5 show examples of the results of tissue0 2D, 5A, and 5D, respectively. In 2D (Fig. 3a), a tumor margin is visible from which the tumor spread gradually from the upper to the lower side; intensity distribution of PpIX corresponded to its tumor distribution (Fig. 3b). Interestingly, intensity at 585 nm was in the

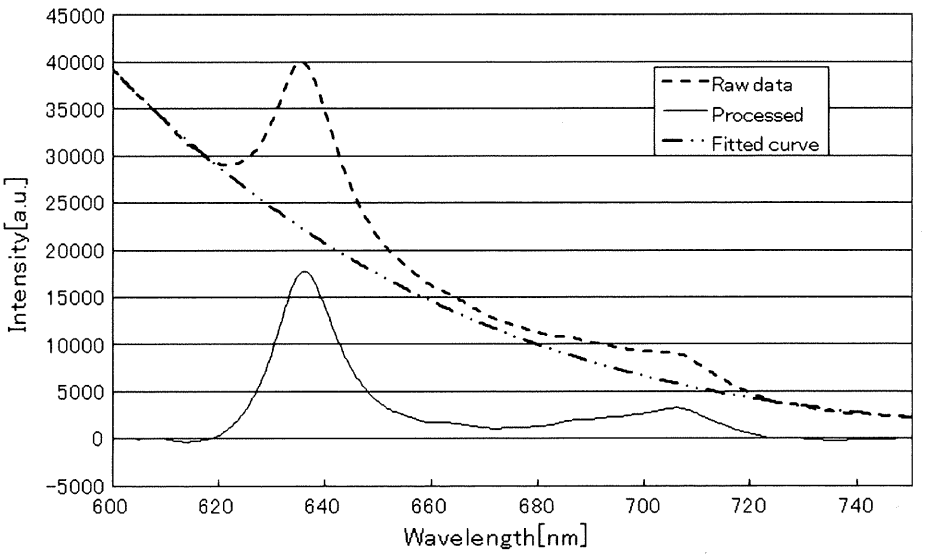

Fig. 2 Background subtraction. *Fitted curve* baseline plotted by the approximate curve of a quartic function. *Raw data* raw spectrum acquired from a specimen. *Processed* processed spectrum plotted by subtracting the base curve from the raw spectrum

opposite distribution (Fig. 3c), which means that the intensity was higher in the normal area (585 nm was determined from the property of a long-pass filter and represents intensity of the short-wavelength side). The peak wavelength seemed almost the same throughout the region (Fig. 3d).

Although tissue 5A had no tumorous cells and seemed to be the region close to the cortex, the tissue had evidence of angiogenesis and gliosis, which can be identified by increased reactive astrocytes (Fig. 4a). Although the tissue was not a tumor, PpIX intensity was as high as that of tumor fluorescence throughout the entire region (Fig. 4b). Therefore, this was a false positive case of fluorescence measurement. However, the 585 nm intensity (Fig. 4c) was higher than that found in other tumor tissues from the same patient. The peak wavelength seemed the same throughout the region (the center region in Fig. 4d shows the error data caused by spectrometer saturation. Because the PpIX spectrum was saturated, the peak wavelength could not be calculated). Tissue 5D was from a tumor margin that had local accumulation of tumor cells (Fig. 5a). PpIX intensity distribution was well correlated with pathological results (Fig. 5b). The intensity of 585 nm had the opposite distribution to PpIX fluorescence (Fig. 5c). Furthermore, the peak wavelength also had a similar distribution (it shifted to the short side at the nontumor region) (Fig. 5d).

Tissue 1 was a tumor margin; the left side was tumor area and the right side the cortex. There was a blood vessel visible at the bottom left corner of the image that emitted strong PpIX fluorescence. However, the intensity at 585 nm was low in the vessel area but high around the vessel. Tissues 2A and 2C showed tumors all over the region, and PpIX intensity was high. Although pathological results showed that tissue 2A was homogeneously tumorous, varied PpIX intensity was observed. Tissue 2C had many vessels on the upper side, and PpIX intensity was relatively high in the region. Tissue 2B was tumorous over the entire tissue area, but only a small portion emitted PpIX fluorescence. Tissue 3A had a tumorous area, but PpIX intensity distribution did not exactly correspond to its tumor area. However, the intensity distribution of 585 nm, which has an opposite distribution to PpIX, was similar to pathological results. Although tissue 3B was not a tumor with blood vessels, PpIX spectrum or any other characteristic spectra were not acquired. Tissue 3C was not tumorous, and PpIX fluorescence was not acquired. Although tissue 4 was tumorous, with tumor cells distributed throughout the entire area, PpIX fluorescence could not be detected over the entire region. Tissue 5B had a nonuniform tumor distribution, including cell characteristics implicating necrosis. This sample might be close to the center of the tumor. PpIX intensity was also nonuniform but showed low intensity around the necrotic area. Tissue 5C was tumor tissue that had diffused astrocytoma cells. PpIX intensity was high over the entire region.

Discussion

In this study, we introduced a novel technique to compare fluorescence spectra distribution of raw tissues with pathological results. We could confirm the necessity of a precise comparison because pathological results showed that cell characteristics varied with location, even when cell size was 5 × 5 mm, as in tissues 2D and 5D. Although we measured only 13 samples in this study, our comparisons showed some trends between spectra and pathological results, which can be divided into three groups. The first group had good correlation between spectra and pathological results, such as in tissues 2D and 5D. Furthermore, three tissues exhibited a relationship between pathological results and intensity distributions at 585 nm and PpIX peak wavelength. As noted earlier, intensity at 585 nm, which represents intensity of the short-wavelength side, has the opposite distribution to PpIX fluorescence. This light may come from an autofluorescence substance such as nicotinamide adenine dinucleotide (NADH), flavin, or lipofuscin [10]. In this study, considering excitation laser wavelength and emission spectrum, lipofuscin and flavin are anticipated to be the autofluorescence substances [11, 12]. Lipofuscin, in particular, appears in neuronal cells of aged patients and exhibits strong fluorescence, with a peak wavelength of approximately 560 nm. These results showed that the precise comparison of spectra with pathological results may increase diagnostic accuracy.

Some specimens, such as tissues 1 and 2C, exhibited high PpIX intensity around blood vessels. Because PpIX accumulates at tumor cells because of BBB disruption, PpIX is thought not to accumulate inside blood vessels. Although the high intensity of PpIX fluorescence was acquired at the blood vessel in tissue 1, the result was thought to be caused by infiltrating tumor around the blood vessel. Unfortunately, in this case, H&E preparation could not reveal the existence of infiltrating tumor cells because the measured point was very local, and preparation fixation was not optimum. In the case of tissue 2C, PpIX fluorescence intensity was relatively high around blood vessels. This result may demonstrate increased 5-ALA intake around blood vessels in which BBB are disrupted, which leads to considerable PpIX accumulation. Although we cannot show conclusive cause, tissue that has blood vessels should be investigated carefully.

The second group comprised false negative cases or cases in which fluorescence distribution was not correlated with pathological findings, such as tissues 2B and 4. There

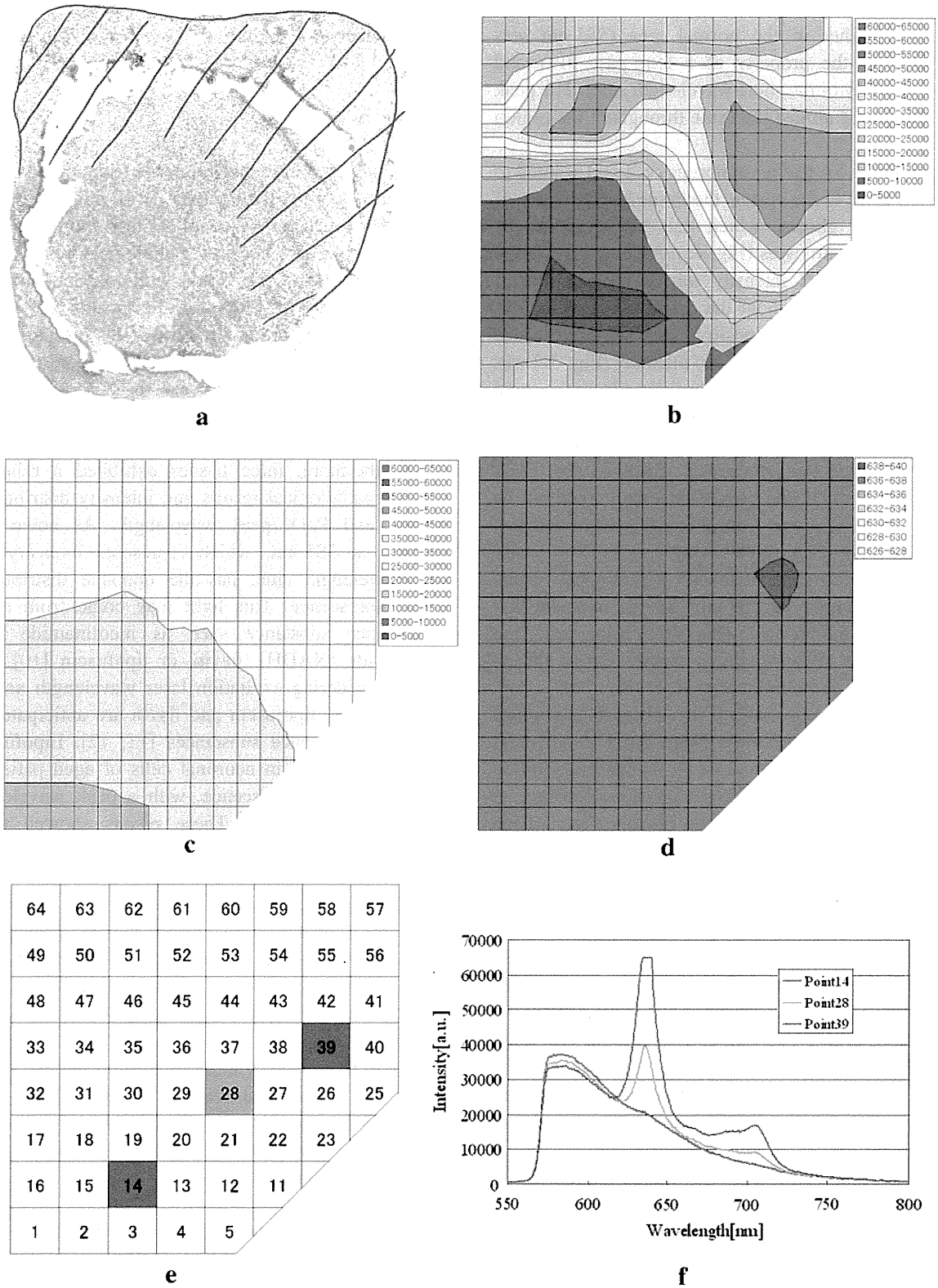

Fig. 3 Results for tissue 2D. **a** Pathological result: this tissue seemed to be the tumor margin. **b** Intensity distribution of protoporphyrin IX (PpIX) fluorescence. **c** Intensity distribution at 585 nm. **d** Peak wavelength distribution of PpIX fluorescence. **e** Examples of measured points. **f** Example of measured spectra corresponding to measured points (**e**)

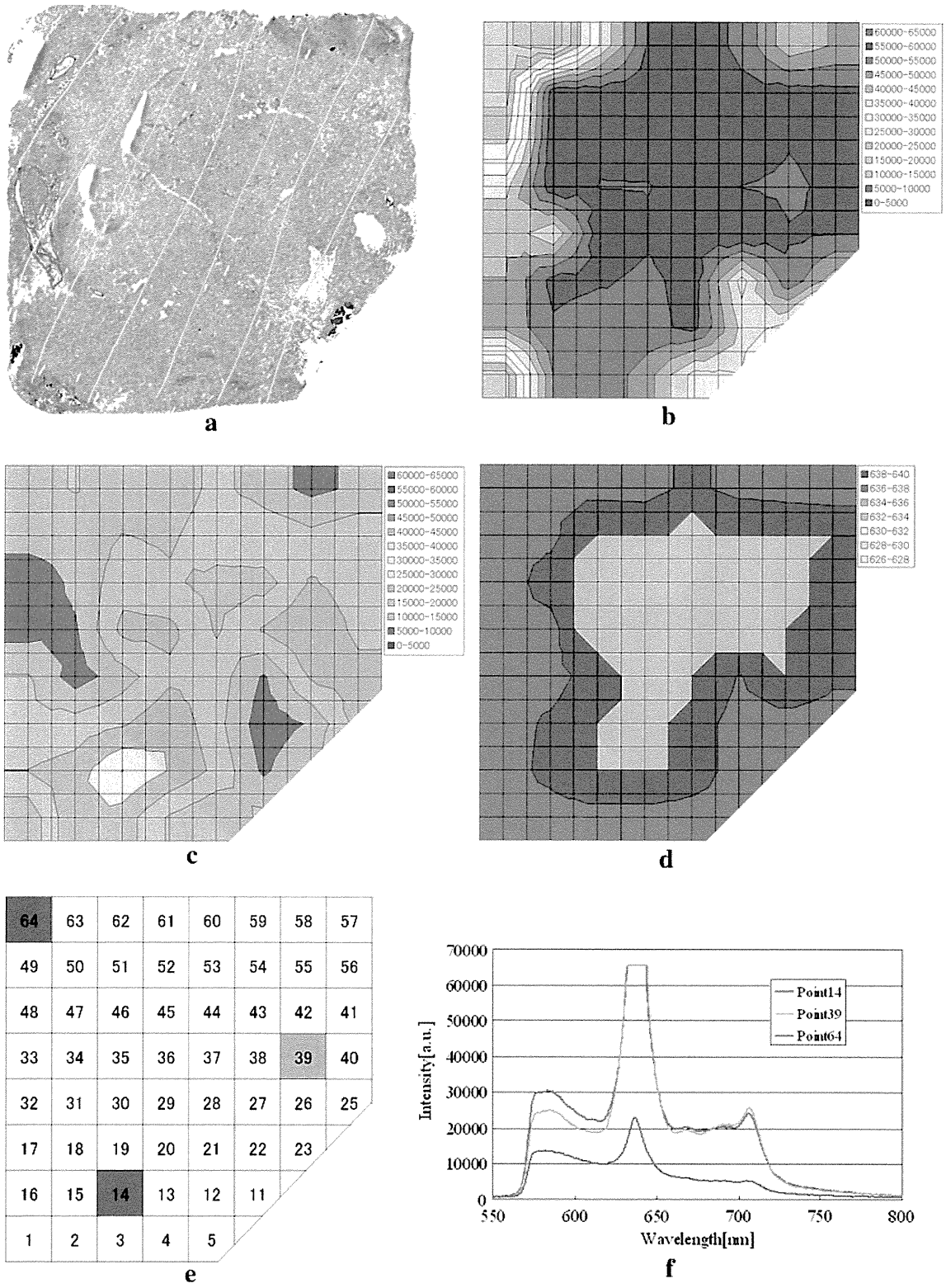

Fig. 4 Results for tissue 5A. **a** Pathological result: this tissue was not tumorous but included reactive astrocytes. **b** Intensity distribution of protoporphyrin IX (PpIX) fluorescence. **c** Intensity distribution at 585 nm. **d** Peak wavelength of distribution of PpIX fluorescence. **e** Examples of measured points. **f** Example of measured spectra corresponding to measured points (**e**)